P-2650

Design of Chopper for Solar Powered Applications

P-2650

A Project Report

Submitted by

Abhishek.M	-	**71205105001**
Mohana Sundaram.N	-	**71205105023**
Sijo Joseph	-	**71205105046**

in partial fulfillment for the award of the degree of

Bachelor of Engineering
in
Electrical & Electronics Engineering

DEPARTMENT OF ELECTRICAL & ELECTRONICS ENGINEERING

KUMARAGURU COLLEGE OF TECHNOLOGY
COIMBATORE – 641 006

ANNA UNIVERSITY: CHENNAI 600 025

APRIL– 2009

Abstract

ABSTRACT

This report summarizes the design of a boost chopper which is triggered based on Maximum Power Point Tracking (MPPT) algorithm, for solar powered applications. The 24V PV array panel is fed to the converter circuit. The chopper circuit steps up the dc voltage level of the panel to 230 V (higher voltage) and maintain the value as constant using the MPPT algorithm for variations in input voltage levels. The MPPT aided closed loop control of chopper for obtaining maximum power point tracking avoids the use of large number of solar arrays connected in series and large capacity storage batteries thereby reducing the cost significantly.

The MPPT algorithm is implemented using the PIC 16F877A Microcontroller in the feedback loop. The dc-dc converter has been fabricated using power MOSFET and associated circuit components. The PIC microcontroller is programmed for automatic variation of the duty cycle of the converter in order to track the maximum power. The simulation of the proposed scheme is done using MATLAB software. The simulation and experimental results are compared and found to be similar.

Acknowledgement

ACKNOWLEDGEMENT

We thank the KCT Management for providing us with all necessary infrastructure and other facilities, to successfully carry out this project.

At the outset, we wish to place on record our sincere thanks and gratitude to **Prof. K. Regupathy Subramanian,** Dean and HOD, Electrical and Electronics Engineering, who motivated us to embark on such a project and whose keen and sustained interest in this project had been a moral booster for us.

We express our deep sense of gratitude and thanks to our project guide **Prof. K. Premalatha,** Electrical and Electronics Engineering department for her valuable guidance with constant encouragement and motivation.

We are indebted to all Teaching and Non-Teaching members of the department of Electrical and Electronics Engineering and other departments for their timely help and valuable suggestions.

Contents

CONTENTS

LIST OF TABLES

LIST OF FIGURES

ABBREVIATIONS

I_{pv}	Current at the operating point of the array (in amps)
I_L	Light-generated current (in amps)
I_o	Reverse Saturation current (in amps)
V_{pv}	Voltage at the operating point of the array (in volts)
R_{se}	Series resistance of the array (in ohms)
A	Thermal voltage (in volts)
I_{sc}	Short-circuit current (in amps)
V_{oc}	Open-circuit voltage of the array (in volts)
L_c	Critical value of inductor in boost chopper (in Henry)
C_c	Critical value of capacitor in boost chopper (in farads)
V_{MPP}	Voltage at Maximum Power Point (in volts)
I_{MPP}	Current at Maximum Power Point (in amps)

Chapter 1

Introduction

1.1 IMPORTANCE OF PV ENERGY

The rapid trend of industrialization of nations and increased interest in environmental issues led to the development of alternative energy systems , which are renewable and pollution free. Among them photovoltaic (PV) power generation system stand out as an important solution. The powerful attraction of the photo voltaic power generation systems is that they produce electric power without inducing environmental pollution by directly transferring solar irradiation into electricity. This fact together with the continuing decrease in the PV array cost (ten fold in the last two decades) and the increase in the efficiency (three fold over the same period) imply promising role for PV generation systems in the near future. Photovoltaic energy is gaining greater visibility during the last several years as a convenient and promising renewable energy source. This has motivated many researchers, scientists and students to pursue their studies in the new developments in this area.

1.2 NEED FOR A BOOST CHOPPER

Due to the fact that solar energy is inconsistent, the regulator is required in most PV application in order to stabilize the fluctuating voltage that they generate. On the other hand most of the electrical appliances are standard with fixed supply voltage such 6, 12, 24 volts etc. There are several types of regulators. The objective of our project is to design a DC-DC Boost converter, which will have the voltage output higher than the input and will be able to couple directly with the inverter (DC-Linked Inverter). The low count of components and simple control circuit of the Boost converter will have the advantage for PV application. The prototype is aimed at high tolerance input voltage with low ripple and stable output voltage at high efficiency.

1.3 REQUIREMENT OF MAXIMUM POWER POINT TRACKING (MPPT) TECHNIQUE

A maximum power point tracker (or MPPT) is a high efficiency DC to DC converter which functions as an optimal electrical load for a photovoltaic (PV) cell, most commonly for a solar panel or array, and converts the power to a voltage or current level which is more suitable to whatever load the system is designed to drive.

1.4 ORGANIZATION OF THE PROJECT WORK

The complete working of the closed loop model of the proposed scheme employing a boost converter is explained in Chapter 2. Simulation studies of the closed loop scheme with MPPT controller is presented in Chapter 3. The hardware requirement and the programming details of firing pulse generation using pic microcontroller are discussed in Chapter 4. A complete experimental set up of the proposed scheme and the experimental results are presented in Chapter 5. The last Chapter summarizes the conclusions of the project and envisages scope for further work.

Chapter 2

MPPT Aided Closed Loop Scheme

2.1 INTRODUCTION

This chapter describes the proposed scheme of maintaining a constant output power to the load implementing a maximum power point tracking on the converter. The power circuit of the boost chopper is presented along with their output waveforms both in continuous and discontinuous mode.

2.2 PROPOSED SCHEME

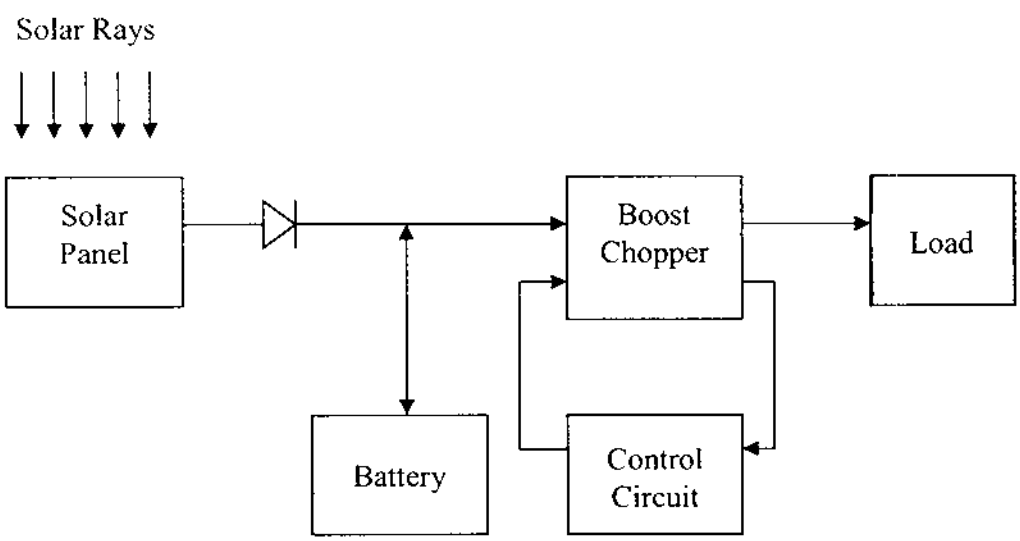

Figure 2.1 Block diagram of the proposed scheme

This scheme employs the following components:

1. PV Panel
2. Storage Battery
3. Boost Chopper
4. Microcontroller based Maximum Power Point Tracking (MPPT) Circuit

The PV panel converts the solar radiation (solar energy) into electrical power that is stored in the storage battery. The voltage stored in the battery is stepped up to higher voltages using the boost chopper. The output voltage or current from the chopper is sensed and is compared with the reference V_{MPP} or I_{MPP} values of the solar panels. If the compared values are found to be different then the MPPT algorithm is

implemented by the PIC microcontroller and the maximum point tracking is performed.

2.3 PV CELL

The physics of the PV cell is very similar to that of the classical diode with a pn junction. When the junction absorbs light, the energy of absorbed photons is transferred to the electron-proton system of the material, creating charge carriers that are separated at the junction. The charge carriers may be electron-ion pairs in a liquid electrolyte or electron-hole pairs in a solid semi conducting material. The charge carriers in the junction region create a potential gradient, get accelerated under the electric field, and circulate as current through an external circuit. The square of the current multiplied by the resistance of the circuit is the power converted into electricity. The remaining power of the photon elevates the temperature of the cell and dissipates into the surroundings.

The origin of the PV potential is the difference in the chemical potential, called the Fermi level, of the electrons in the two isolated materials. When they are joined, the junction approaches a new thermodynamic equilibrium. Such equilibrium can be achieved only when the Fermi level is equal in the two materials. This occurs by the flow of electrons from one material to the other until a voltage difference is established between them, which has a potential just equal to the initial difference of the Fermi level. This potential drives the photocurrent in the PV circuit.

Metallic contacts are provided on both sides of the junction to collect electrical current induced by the impinging photons. A thin conducting mesh of silver fibers on the top (illuminated) surface collects the current and lets the light through. The spacing of the conducting fibers in the mesh is a matter of compromise between maximizing the electrical conductance and minimizing the blockage of the light. Conducting-foil (solder) contact is provided over the bottom (dark) surface and on one edge of the top surface. In addition to the basic elements, several enhancement features are also included in the construction.

2.4 MODULE AND ARRAY

The solar cell described in the preceding subsection is the basic building block of the PV power system. Typically, it is a few square inches in size and produces about 1W of power. To obtain high power, numerous such cells are connected in series and parallel circuits on a panel (module) area of several square feet. The solar array or panel is defined as a group of several modules electrically connected in a series-parallel combination to generate the required current and voltage.

Mounting the modules can be in various configurations. In roof mounting, the modules are in a form that can be laid directly on the roof. In the newly developed amorphous silicon technology, the PV sheets are made in shingles that can replace the traditional roof shingles on a one-to-one basis, providing better economy in regard to building material and labor.

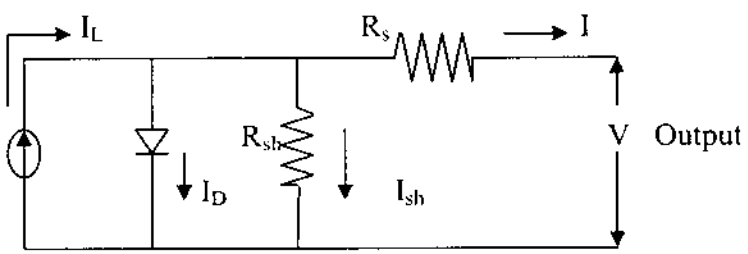

Figure 2.2 Equivalent circuit of the PV Cell

2.5 CHARACTERISTICS OF SOLAR CELL

A solar cell or photovoltaic cell is a machine that converts sunlight directly into electricity by the photovoltaic effect. Sometimes the term solar cell is reserved for devices intended specifically to capture energy from sunlight, while the term photovoltaic cell is used when the source is unspecified. Assemblies of cells are used to make solar panels, solar modules, or photovoltaic arrays. Photovoltaic is the field of technology and research related to the application of solar cells in producing electricity for practical use. The energy generated this way is an example of solar energy (also called solar power).

The voltage, current and power delivered by the solar cell are influenced by

1) Conditions of sunlight, intensity, wavelength, angle of incidence
2) Conditions of the junction temperature.
3) External resistance

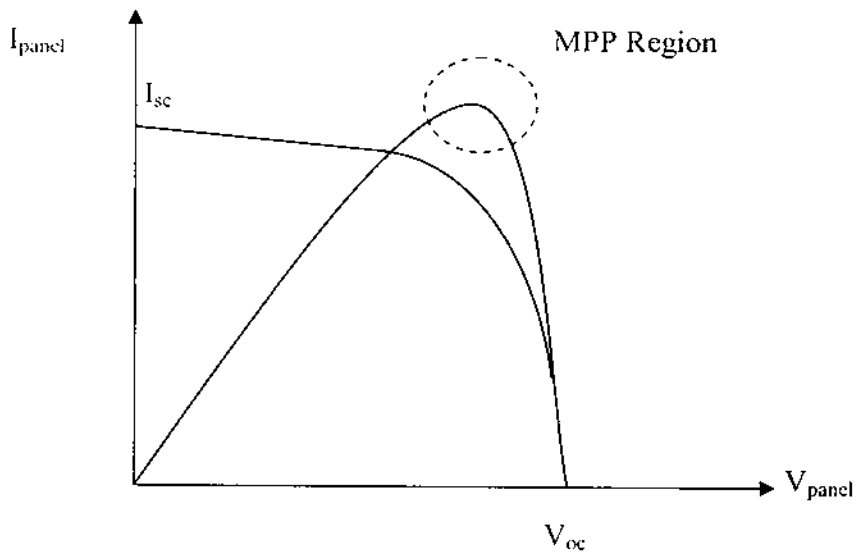

Figure 2.3 Characteristics of Solar cell

When the external resistance is very high (Mega Ohms) the condition is called an open circuit. The open circuit voltage Voc, is the maximum voltage across a PV cell; the open circuit current is zero. If the external resistance is reduced gradually and the readings of the terminal voltage V and load current I are taken, we get the VI characteristics of the PV cell. When the external resistance is completely shorted, the condition is called the short circuit. The short circuit current Isc is the maximum current across the PV cell; the short circuit voltage is zero.

2.6. BOOST CHOPPER

A boost converter (step-up converter) is a power converter with an output DC voltage greater than its input DC voltage. It is a class of switching-mode power supply (SMPS) containing at least two semiconductor switches (a diode and a transistor) and at least one energy storage element. Filters made of capacitors (sometimes in combination with inductors) are normally added to the output of the converter to reduce output voltage ripple.

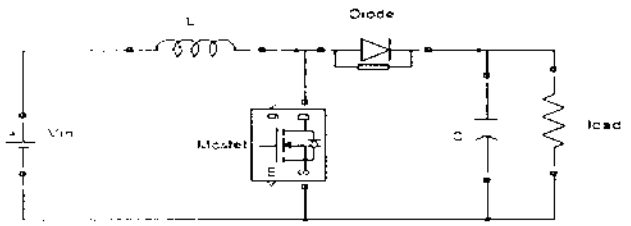

Figure 2.4 Basic Circuit of Boost Chopper

2.6.1 Basic Operation

Boost chopper using the power MOSFET is shown in the figure. The circuit operation can be divided into two modes. Mode 1 begins when transistor M_1, is switched on at t=0. The input current, which rises, flows through inductor L, and transistor. Mode 2 begins when transistor M_1 is switched of at $t=t_1$. The current which was flowing through the transistor would now flow through L, C, load and diode D_m. The inductor current falls until transistor M1 is turned on again in the next cycle. The energy stored in inductor L is transferred to the load. The equivalent circuits for the modes of operation and the output waveforms for voltages and currents are also shown in the figure.

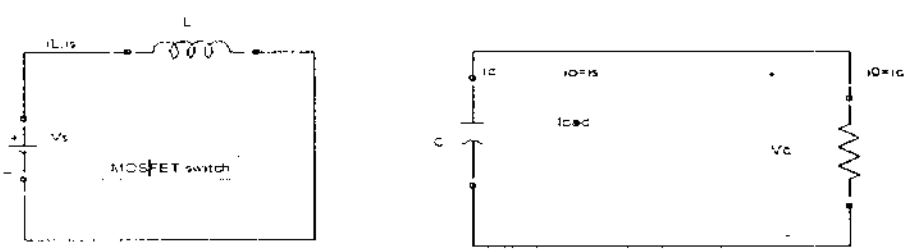

Mode I

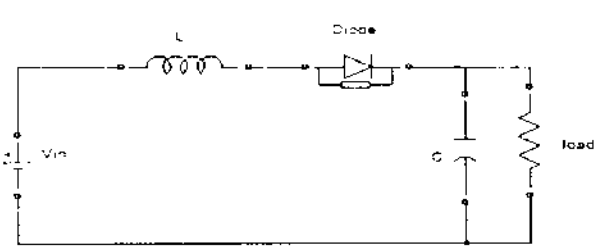

Mode 2

Figure 2.5 Equivalent Circuits of Boost Chopper

If V_s is the supply voltage and k is the duty cycle ratio then,

Average output voltage, V_a = Vs/(1-k)

Duty cycle ratio, k = T_{on} / T

If V_s= 24V, V_a=230V, f=50 KHz ; then the design values are :

1-k = (V_s / V_a) = 24/230 = 0.104

k = 0.896 = 89.6%

L_c = ((1-k)*k*R/(2*f)) = (0.104*0.896*50)/(2*50*10^3)

= 0.078 H

C_c = (k/(2*f*R)) = (0.896/(2*50*10^3*50))

= 1250 microF

A boost regulator can step up the output voltage without a transformer. Due to single transistor, it has a high efficiency.

2.6.2. Waveforms of Boost Converter

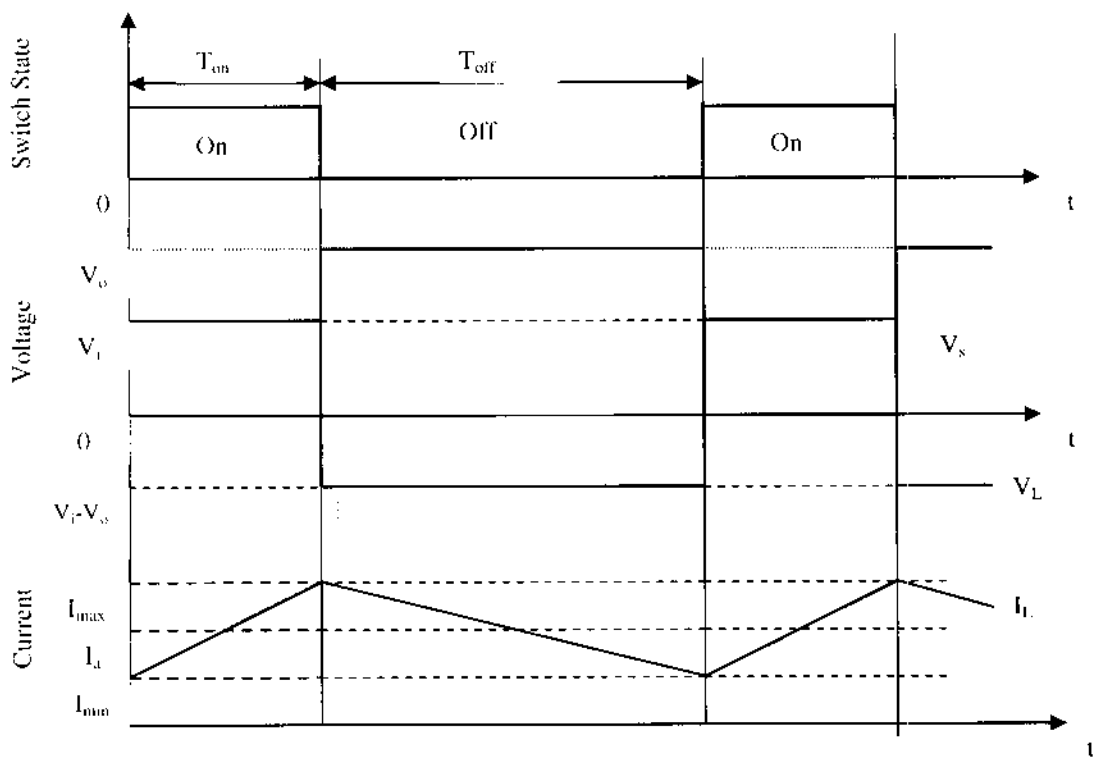

Figure 2.6 Current and Voltage Waveforms of Boost converter(continuous mode)

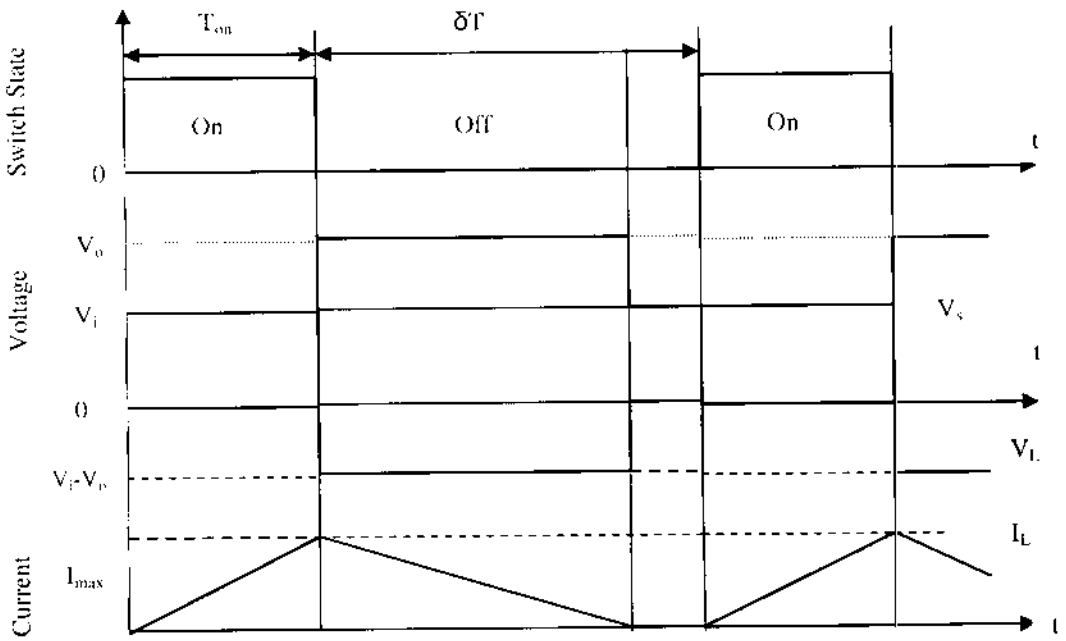

Figure 2.7 Current and Voltage Waveforms of Boost converter(discontinuous mode)

2.6.3 Applications of Boost Converter

Battery powered systems often stack cells in series to achieve higher voltage. However, sufficient stacking of cells is not possible in many high voltage applications due to lack of space. Boost converters can increase the voltage and reduce the number of cells. Two battery-powered applications that use boost converters are hybrid electric vehicles (HEV) and lighting systems. Boost converters also power devices at smaller scale applications, such as portable lighting systems. A white LED typically requires 3.3V to emit light, and a boost converter can step up the voltage from a single 1.5 V alkaline cell to power the lamp. Boost converters can also produce higher voltages to operate cold cathode fluorescent tubes (CCFL) in devices such as LCD backlights and some flashlights.

2.7 MAXIMUM POWER POINT TRACKING TECHNIQUES

2.7.1 Fractional Open-Circuit Voltage

The near linear relationship between V_{MPP} and V_{OC} of the PV array, under varying irradiance and temperature levels, has given rise to the fractional V_{OC} method

$V_{MPP} \approx k1 V_{OC}$, where k1 is a constant of proportionality. Since k1 is dependent on the characteristics of the PV array being used, it usually has to be computed beforehand by empirically determining V_{MPP} and V_{OC} for the specific PV array at different irradiance and temperature levels. The factor k1 has been reported to be between 0.71 and 0.78. Once k1 is known, V_{MPP} can be computed using the above equation with V_{OC} rating of the panel. The output voltage of the chopper circuit is compared with V_{MPP} value. A closed loop control to maintain the output voltage constant is provided by the microcontroller based MPPT tracker.

2.7.2 Fractional Short-Circuit Current

Fractional I_{SC} results from the fact that, under varying atmospheric conditions, I_{MPP} is approximately linearly related to the I_{SC} of the PV array $I_{MPP} \approx k2 I_{SC}$ where k2 is a proportionality constant. Just like in the fractional V_{OC} technique, k2 has to be determined according to the PV array in use. The constant k2 is generally found to be between 0.78 and 0.92. Once k2 is known, I_{MPP} can be calculated using the above equation using the I_{SC} rating of the panel. As in the previous method, here the output current from the boost chopper is compared with the I_{MPP} value. A closed loop control to maintain the output current constant is provided by the microcontroller based tracking.

2.7.3. Load Current or Load Voltage Maximization

The purpose of MPPT techniques is to maximize the power coming out of a PV array. When the PV array is connected to a power converter, maximizing the PV array power also maximizes the output power at the load of the converter. Conversely, maximizing the output power of the converter should maximize the PV array power, assuming a lossless converter. The loads are mostly voltage-source type, current-source type, resistive type, or a combination of these. For a voltage-source type load, the load current I_{out} should be maximized to reach the maximum output power P_M. For a current-source type load, the load voltage V_{out} should be maximized. For the other load types, either I_{out} or V_{out} can be used. This is also true for nonlinear load types as long as they do not exhibit negative impedance characteristics . Therefore, for almost

all loads of interest, it is adequate to maximize either the load current or the load voltage to maximize the load power. Consequently, only one sensor is needed. In most PV systems, a battery is used as the main load or as a backup. Since a battery can be thought of as a voltage-source type load, the load current can be used as the control variable. Positive feedback is used to control the power converter such that the load current is maximized and the PV array operates close to the MPP. Operation exactly at the MPP is almost never achieved because this MPPT method is based on the assumption that the power converter is lossless.

2.8 MPPT TECHNIQUE - FLOWCHART

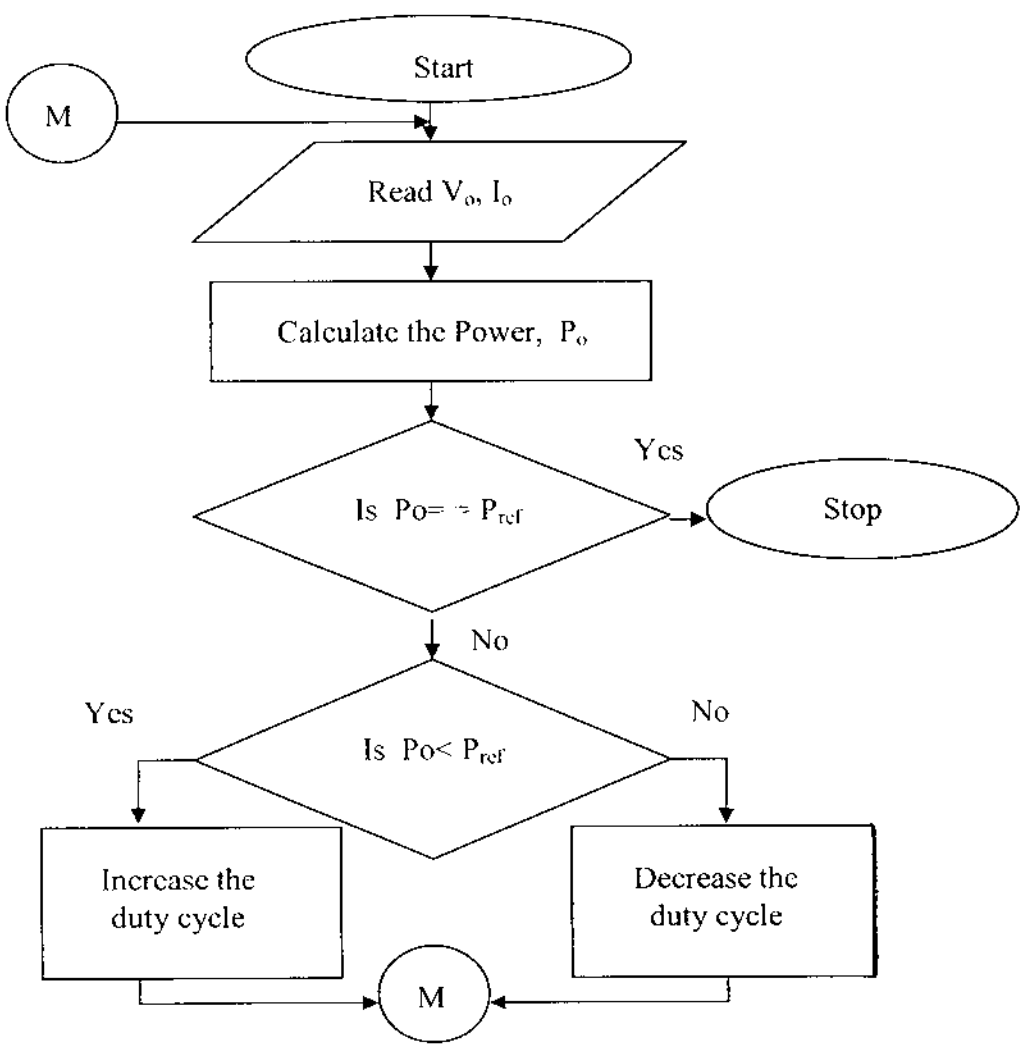

Figure 2.8 Flowchart of MPPT algorithm

Chapter 3

Simulation Modeling and Results of the Closed Loop Scheme

3.1 INTRODUCTION

In this chapter, the simulation model of the proposed closed loop scheme and other simulation related aspects are discussed. MATLAB software is used for simulating the circuit. The arrangements of different components and the procedure for simulation are presented below. The circuit is simulated for different input voltage levels such that the output voltage is maintained constant.

3.2 AN OVERVIEW OF MATLAB SOFTWARE

MATLAB is a numerical computing environment and programming language. MATLAB allows easy matrix manipulation, plotting of functions and data, implementation of algorithms, creation of user interfaces, and interfacing with programs in other languages, although it is numeric only. An additional package, Simulink, adds graphical multi domain simulation and Model-Based Design for dynamic and embedded systems. In 2004, Math Works claimed that MATLAB was used by more than one million people across industry and the academic world.

MATLAB is one of the fastest and most enjoyable ways to solve problems numerically. The computational problems arising in most undergraduate courses can be solved much more quickly with MATLAB, than with the standard programming languages (Fortran, C, Java, etc.). It is particularly easy to generate some results, draw graphs to look at the interesting features, and then explore the problem further. By minimizing human time, MATLAB is particularly useful in the initial investigation of real problems; even though they may eventually have to be solved using more computationally efficient ways on super computers.

3.3 PROCEDURE FOR SIMULATION USING MATLAB

The steps that are to be followed for simulating the circuit using MATLAB are given below:

- The Model window is opened and the components are placed from the library browser and the parameters of each and every component are specified.
- A resistive load is connected at the output of the chopper

- The Scope is connected for viewing the input and output voltage levels.

3.3.1 PV Array Model:

The classical equation of a PV cell describes the relationship between current I_{pv} and voltage V_{pv} of the cell as

$$I_{pv} = I_L - I_o [\exp\{(V_{pv} + R_{se}I_{pv}) / A\} - 1] \quad \ldots\ldots\ldots\ldots\ldots (1)$$

Assuming,

$$\exp \{(V_{pv} + R_{se}I_{pv})/A\} >> 1,$$

$$I_o/I_{sc} \approx 10^{-9}$$

and $I_L \cdot I_{sc}$.

Equation (1) can be written as $I_{pv} = I_{sc} - I_d$ ..... (2)

where $I_d = 10^{-9} I_{sc} [\exp \{(20.7/V_{oc})*(V_{pv} + R_{se}I_{pv})\}]$ .....(3)

since $V_{pv\ ;Ipv=0} = Voc$.

The above equations can be used to determine the characteristics of a panel or an array, as it is evident that the characteristics of a panel made up of identical cells can be obtained by appropriately scaling the V-I characteristics of the individual cells.

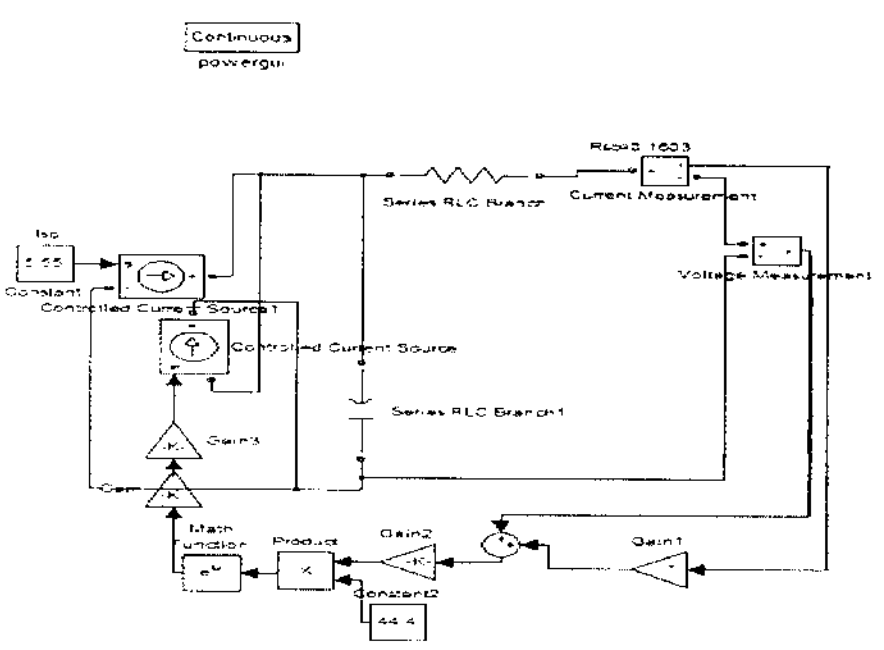

Figure 3.1 PV Array Model developed using MATLAB

3.3.2. Simulation Circuit

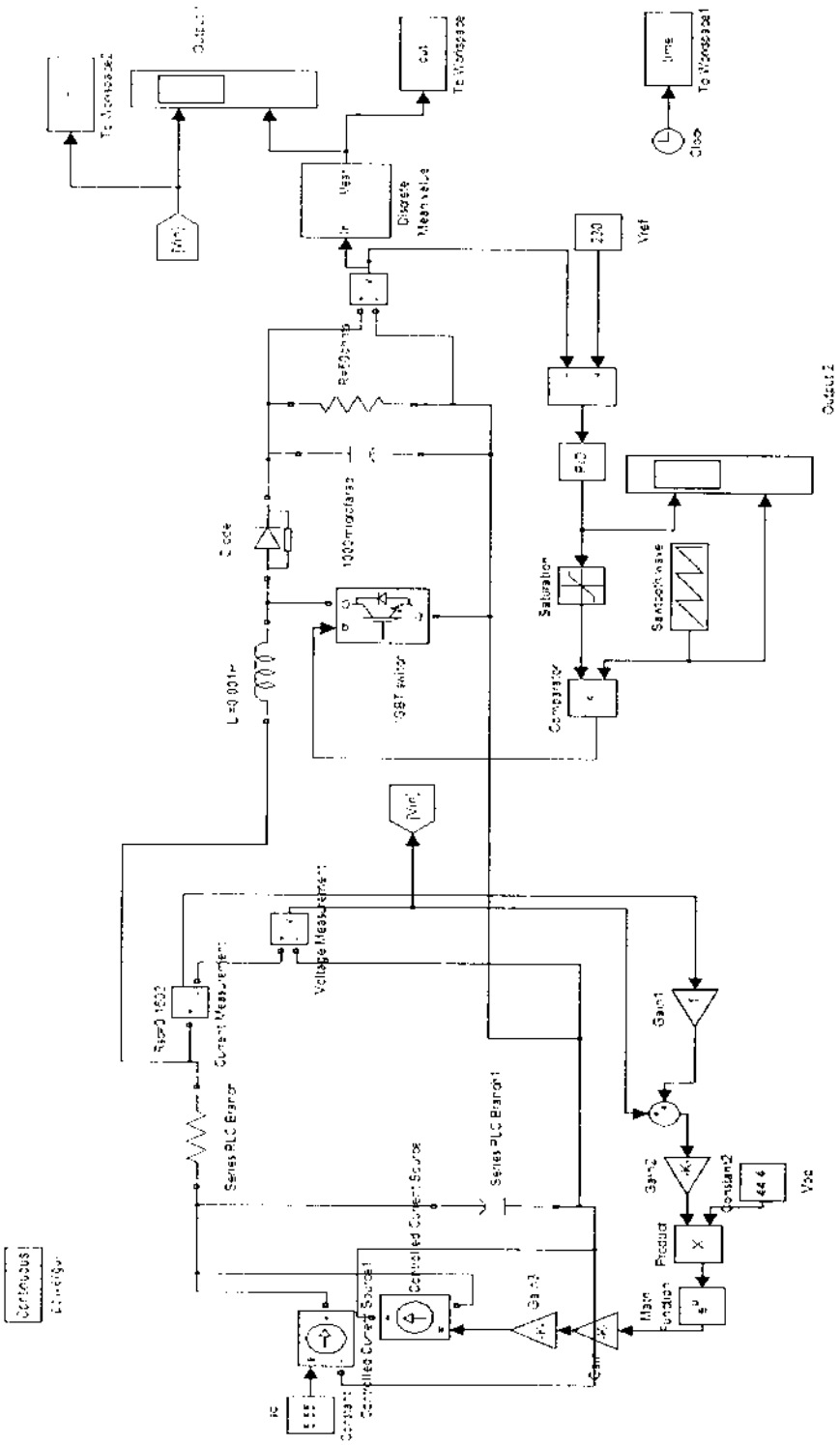

Figure 3.2 Simulation Circuit with PV Array Model

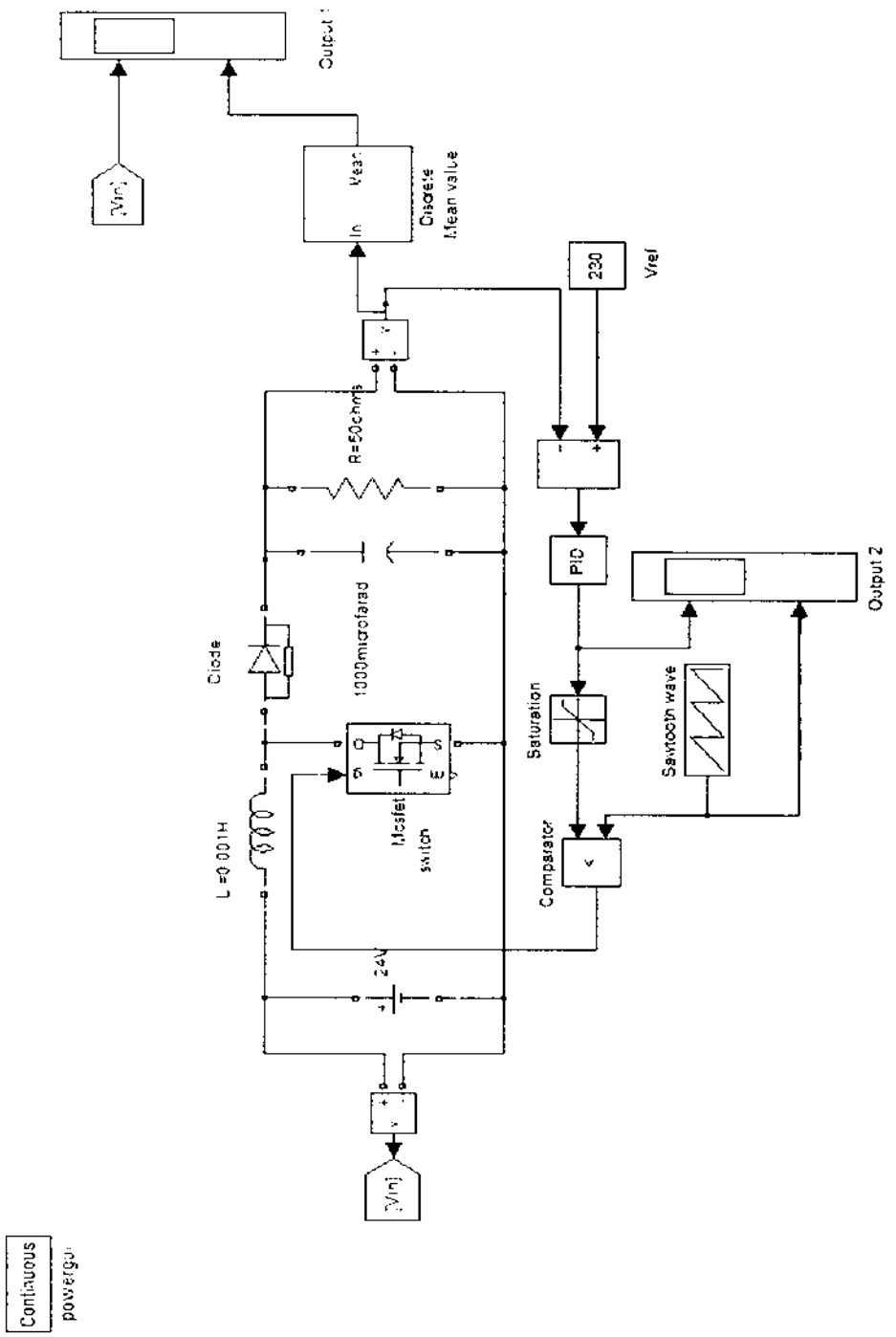

Figure 3.3 Simulation Circuit with DC Source

In the simulation circuit, the PV array model developed using panel's open circuit voltage and short circuit current, is used as an input source. The boost chopper is constructed using 1mH Inductor, a Mosfet and a capacitor of 1000μF. The output is sensed by a voltmeter and is compared with a reference voltage. The reference voltage is determined based on open circuit voltage of solar panel, which is discussed in Chapter 2. A PI (Proportional-Integral) Controller which causes the steady state error to be zero, is used with the values proportional constant, P=10 and integral constant, I=2.

The output of the controller is passed through the saturation zone. The saturation zone limits the input signal to upper and lower saturation values. The values specified in saturation zone block are +0.5 and -0.5 as upper and lower saturation limit respectively. The result is compared with the saw tooth waveform. The saw tooth waveform block outputs a repeating sequence of number specified and the value of time is monotonically increased. The compared result is connected to the gate terminal of Mosfet, thereby causing trigger. When the input voltage varies, the compared result also varies accordingly. In this way, the output voltage is maintained constant in spite of changes in the input. A resistive load of 50 Ohms is connected across the chopper output.

The 24V PV panel array is used as the input source to the boost chopper. In the simulation circuit, in order to show the variations in the input voltage levels, the PV panel is replaced by DC voltage sources of different values.

3.3.3 Simulation results

- After constructing the circuit, the required simulation time is specified and the simulation is started.
- Since, the output voltage has to be maintained constant for varying input voltages, the simulation is tried for varying input voltages.
- The input and output waveforms for different input voltage levels (24V, 20V and 30V) are shown below.

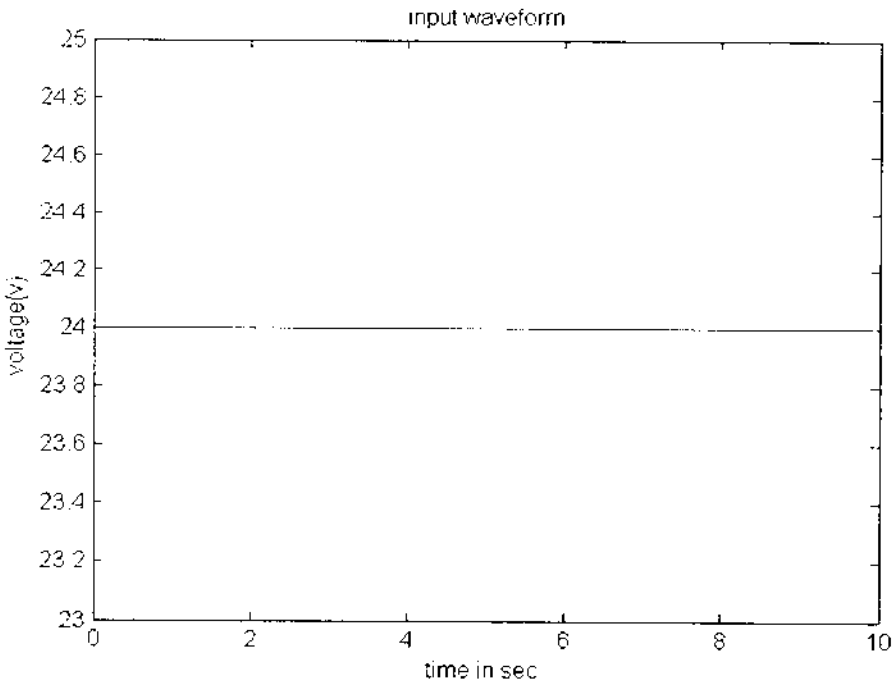

Figure 3.4 24V Input Voltage waveform

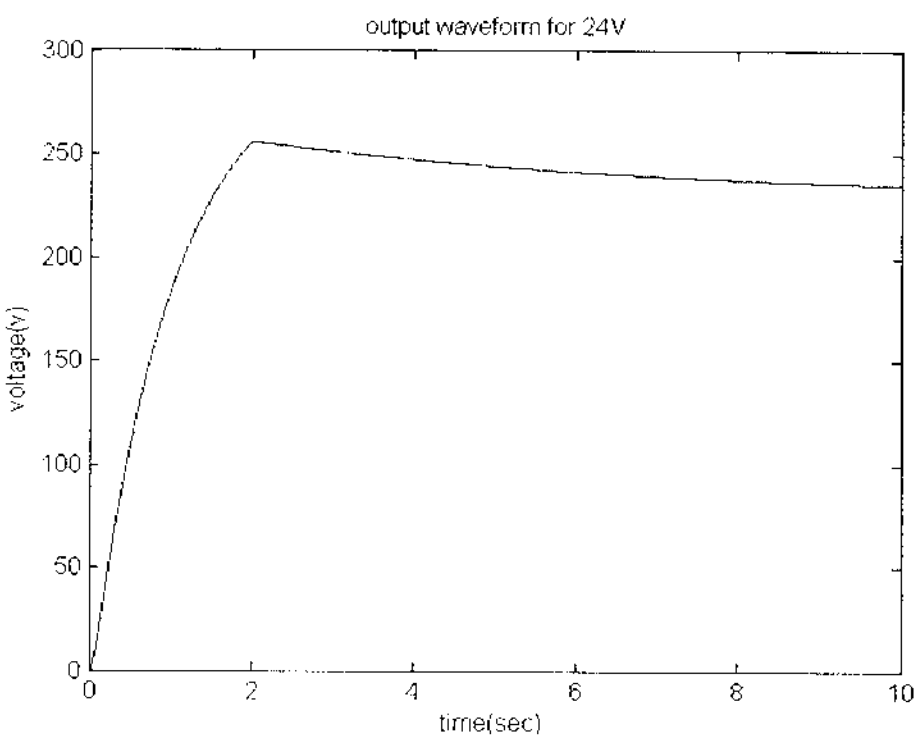

Figure 3.5 Output Voltage waveform for 24V input

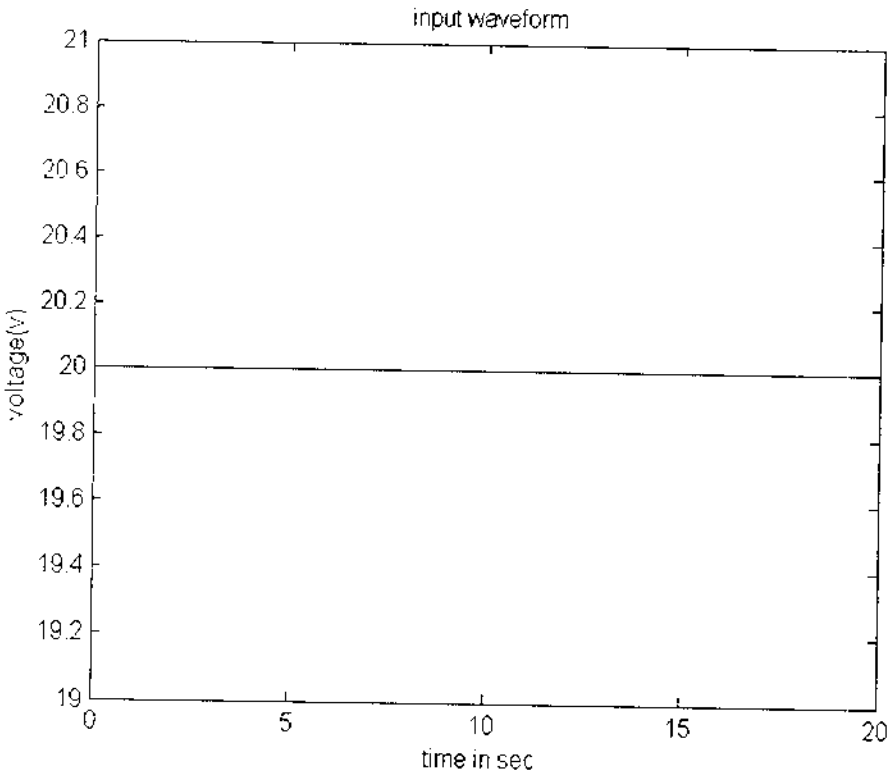

Figure 3.6 20V Input Voltage waveform

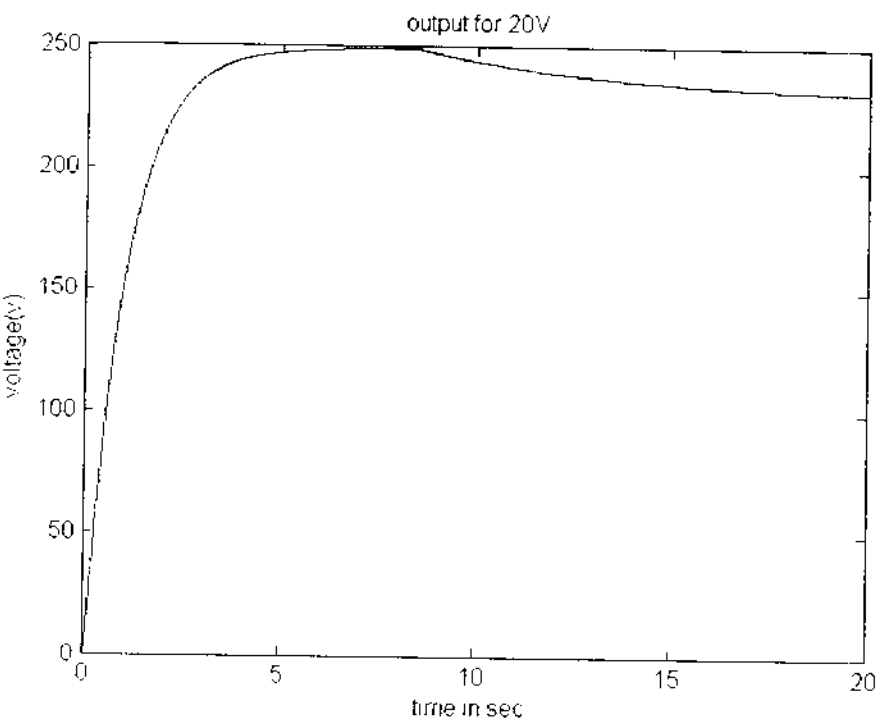

Figure 3.7 Output Voltage waveform for 20V input

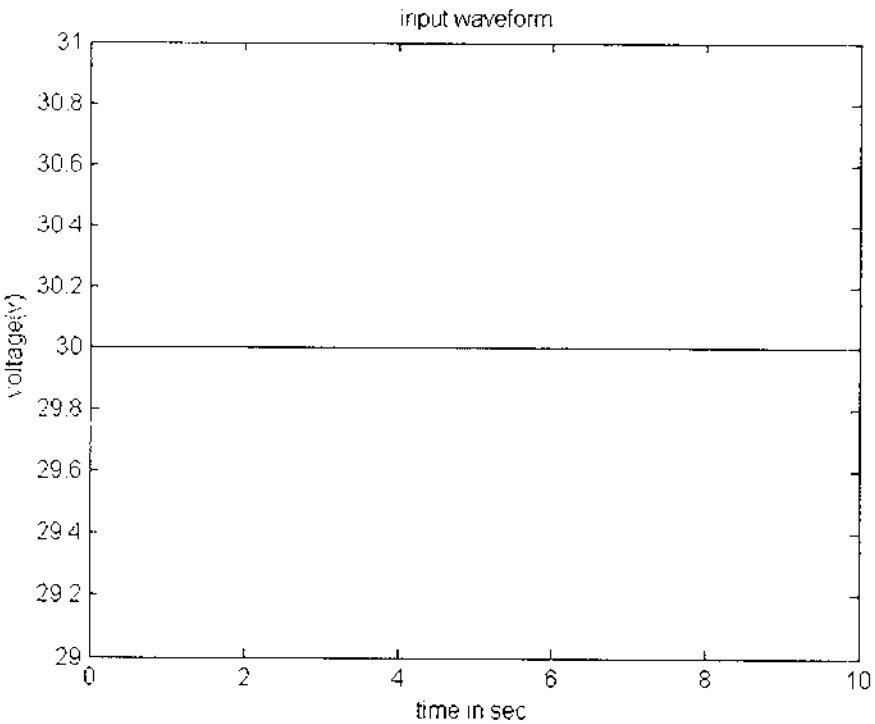

Figure 3.8 30V Input Voltage waveform

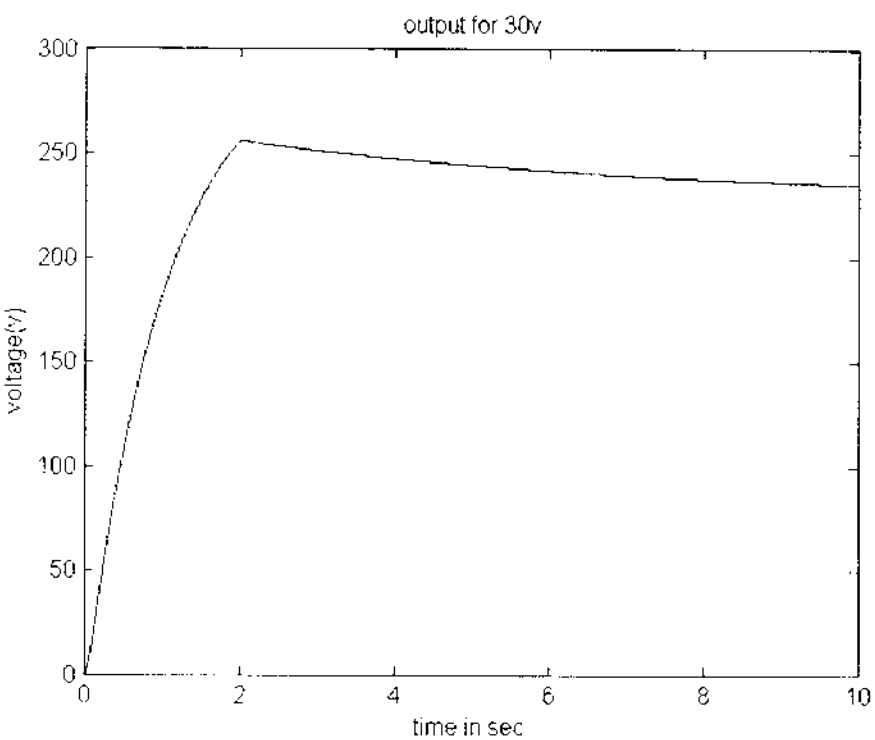

Figure 3.9 Output Voltage waveform for 30V input

4.1 INTRODUCTION

For generating gate pulse to the MOSFET in the converter, either a microprocessor or microcontroller scheme can be effectively used. Of the two schemes, the microcontroller based one is more compact as it requires less hardware and is also more reliable. In the present project, a low cost, high performance PIC 16F877A has been used for generating the gate pulse to the MOSFET in the dc-dc converter. The details of the hardware required for the pulse generation are described in this chapter.

4.2 NEED FOR MICRO CONTROLLER BASED PWM GENERATION

- Micro controller has inbuilt functions such as timer, ADC, PWM, oscillator which reduce the hardware components used.
- PWM technique used enables the reduction of harmonics
- Wide variation in speed since frequency is used as control parameter.
- Digital circuits used employ a faster response.
- Automatic speed control is achieved since no manual parts are involved.
- The Micro controller IC Chip senses the input speed requirement and gives the output in favor of the input.
- No external commutation circuits are required.

4.3 PIC MICROCONTROLLER

PIC16F877A is a small piece of semiconductor integrated circuits. The package type of these integrated circuits is DIP package. DIP stand for Dual Inline Package for semiconductor IC. This package is very easy to be soldered onto the strip board. However using a DIP socket is much easier so that this chip can be plugged and removed from the development board.

This IC can be reprogrammed and erased up to 10,000 times. Therefore it is very good for new product development phase.

16F877A PIC Microcontroller is used for controlling the width of the pulses from PWM generator, by fixing either the frequency or voltage so that the MOSFETs are turned ON and OFF in the desired sequence.

4.3.1 Core Features

- High-performance RISC CPU
- Only 35 single word instructions to learn
- Operating speed: DC - 20 MHz clock input
  DC - 200 ns instruction cycle
- Up to 8K x 14 words of Flash Program Memory,
  Up to 368 x 8 bytes of Data Memory (RAM)
  Up to 256 x 8 bytes of EEPROM data memory
- Interrupt capability (up to 14 internal/external)
- Eight level deep hardware stack
- Direct, indirect, and relative addressing modes
- Power-on Reset (POR)
- Power-up Timer (PWRT) and Oscillator Start-up Timer (OST)
- Watchdog Timer (WDT) with its own on-chip RC Oscillator for reliable operation
- Programmable code-protection
- Power saving SLEEP mode
- Selectable oscillator options
- In-Circuit Serial Programming (ICSP) via two pins
- Only single 5V source needed for programming capability
- In-Circuit Debugging via two pins
- Wide operating voltage range: 2.5V to 5.5V
- High Sink/Source Current: 25 mA
- Commercial and Industrial temperature ranges
- Low-power consumption:
  < 2 mA typical @ 5V, 4 MHz
  20mA typical @ 3V, 32 kHz
  < 1mA typical standby current

4.3.2 Peripheral Features

- 33 I/O pins: 5 I/O ports
- Timer0: 8-bit timer/counter with 8-bit prescaler
- Timer1: 16-bit timer/counter with prescaler
  - Can be incremented during Sleep via external crystal/clock
- Timer2: 8-bit timer/counter with 8-bit period register, prescaler and postscaler
- Two Capture, Compare, PWM modules
  - 16-bit Capture input; max resolution 12.5 ns
  - 16-bit Compare; max resolution 200 ns
  - 10-bit PWM
- Synchronous Serial Port with two modes:
  - SPI Master
  - I2C Master and Slave
- USART/SCI with 9-bit address detection
- Parallel Slave Port (PSP)
  - 8 bits wide with external RD, WR and CS controls
- Brown-out detection circuitry for Brown-Out Reset

4.3.3 Analog Features

- 10-bit, 8-channel A/D Converter
- Brown-Out Reset
- Analog Comparator module
  - 2 analog comparators
  - Programmable on-chip voltage reference module
  - Programmable input multiplexing from device inputs and internal VREF
  - Comparator outputs are externally accessible

4.3.4 Architecture of PIC 16F877A

Device	Program Flash	Data Memory	Data EEPROM
PIC16F874	4K	192 Bytes	128 Bytes
PIC16F877	8K	368 Bytes	256 Bytes

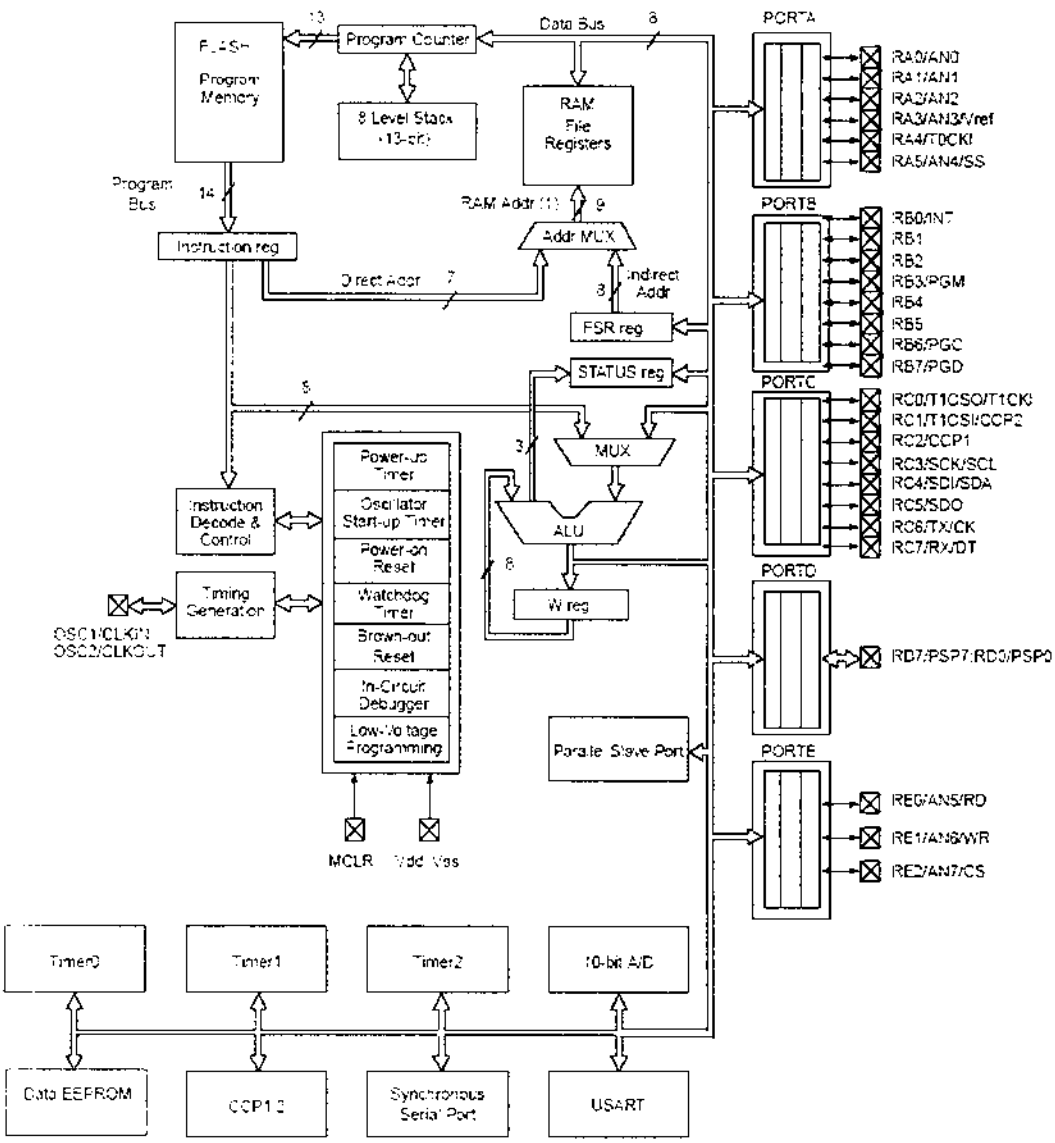

Note 1. Higher order bits are from the STATUS register

Figure 4.1 .Architecture of PIC 16F877A Microcontroller

4.3.5 PIC 16F877A Microcontroller Pin Diagram

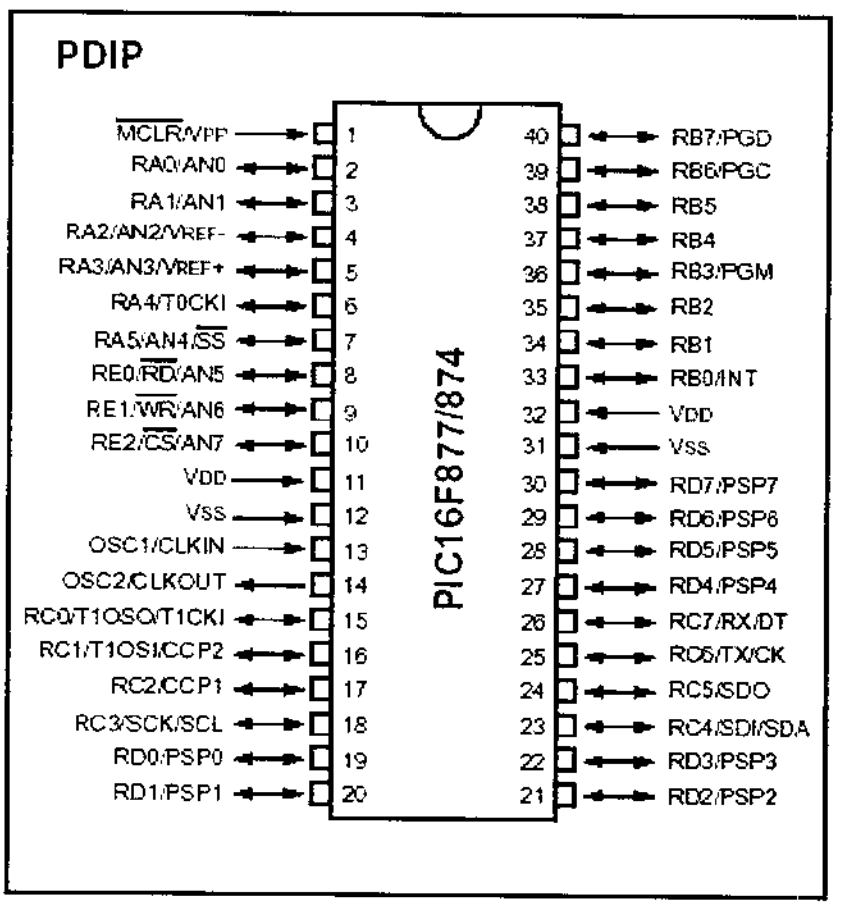

Figure 4.2 Pin diagram of PIC 16F877 Microcontroller

Figure 4.2 shows the pin out diagram of the PIC 16F877 Microcontroller. It is a 40 pin dual inline package(DIP) IC. It has five input / output ports named as Port A, Port B, Port C, Port D and Port E .

Some pins for these I/O ports are multiplexed with an alternate function for the peripheral features on the device. In general, when a peripheral is enabled, that pin may not be used as a general purpose I/O pin.

4.3.6 Analog-to-Digital Converter (A/D) Module

The Analog-to-Digital (A/D) Converter module has five inputs for the 28-pin devices and eight for the 40/44-pin devices. The conversion of an analog input signal results in a corresponding 10-bit digital number. The A/D converter has a unique feature of being able to operate while the device is in Sleep mode. To operate in Sleep, the A/D clock must be derived from the A/D's internal RC oscillator. The A/D module has four registers.

The registers are:

- A/D Result High Register (ADRESH)
- A/D Result Low Register (ADRESL)
- A/D Control Register 0 (ADCON0)
- A/D Control Register 1 (ADCON1)

4.3.6.1. Adcon0 Register (Address 1fh)

The ADCON0 register, controls the operation of the A/D module. The ADCON1 register configures the functions of the port pins. The port pins can be configured as analog inputs or as digital I/O.

R/W-0	R/W-0	R/W-0	R/W-0	R/W-0	R/W-0	U-0	R/W-0
ADCS1	ADCS0	CHS2	CHS1	CHS0	GO/DONE	-----	ADON
bit 7							bit 0

Figure 4.3 ADCON0 Register

bit 7-6 ADCS1:ADCS0: A/D Conversion Clock Select bits

Table 4.1 A/D Conversion Clock Select bits for ADCON0 Register

ADCON1 <ADCS2>	ADCON0 <ADCS1:ADCSO>	Clock Conversion
0	00	Fosc/2
0	01	Fosc/8
0	10	Fosc/32

0	11	F_{RC} (clock derived from the internal A/D RC oscillator)
1	00	Fosc/4
1	01	Fosc/16
1	10	Fosc/64
1	11	F_{RC} (clock derived from the internal A/D RC oscillator)

bit 5-3 CHS2:CHS0: Analog Channel Select bits

000 = Channel 0 (AN0)

001 = Channel 1 (AN1)

010 = Channel 2 (AN2)

011 = Channel 3 (AN3)

100 = Channel 4 (AN4)

101 = Channel 5 (AN5)

110 = Channel 6 (AN6)

111 = Channel 7 (AN7)

bit 2 GO/DONE: A/D Conversion Status bit. When ADON=

1 = A/D conversion in progress (setting this bit starts the A/D conversion which is automatically cleared by hardware when the A/D conversion is complete)

0 = A/D conversion not in progress

bit 1 Unimplemented: Read as '0'

bit 0 ADON: A/D On bit

1 = A/D converter module is powered up

0 = A/D converter module is shut-off and consumes no operating current

ADCON0 allows setting the conversion clock time, channel selection, to observe the conversion status and AD module ON/OFF control. ADCON0 is at address 1FH, which is in bank0 of 16F87X register file map.

4.3.6.2. Adcon1 Register (Address 9fh)

ADCON1 allows selecting the AD conversion result format (right or left justification), the PORT A bits for analog or digital use. ADCON1 is at address 9FH, which is in bank1. ADCON1 bits 0 to 3 define the analog or digital use of PORT A pins. If these bits are 0000, then all PORTA pins are configured as all for analog purpose. The corresponding data direction registers must be defined for making PORTA pins as input.

R/W-0	R/W-0	U-0	U-0	R/W-0	R/W-0	R/W-0	R/W-0
ADFM	ADCS2	------	------	PCFG3	PCFG2	PCFG1	PCFG0
bit 7							bit 0

Figure 4.4 ADCON1 Register

bit 7 ADFM: A/D Result Format Select bit

1 = Right justified. Six (6) Most Significant bits of ADRESH are read as '0'.

0 = Left justified. Six (6) Least Significant bits of ADRESL are read as '0'.

bit 6 ADCS2: A/D Conversion Clock Select bit

Table 4.2 A/D Conversion Clock Select bit for ADCON1 Register

ADCON1 <ADCS2>	ADCON0 <ADCS1:ADCSO>	Clock Conversion
0	00	Fosc/2
0	01	Fosc/8
0	10	Fosc/32
0	11	F_{RC} (clock derived from the internal A/D RC oscillator)
1	00	Fosc/4
1	01	Fosc/16
1	10	Fosc/64
1	11	F_{RC} (clock derived from the internal A/D RC oscillator)

bit 5-4 Unimplemented: Read as '0'

bit 3-0 PCFG3:PCFG0: A/D Port Configuration Control bits

Table 4.3 A/D Port Configuration Control bits for ADCON1 Register

PCFG <3:0>	AN7	AN6	AN5	AN4	AN3	AN2	AN1	AN0	V_{REF+}	V_{REF-}	C/R
0000	A	A	A	A	A	A	A	A	V_{DD}	V_{SS}	8/0
0001	A	A	A	A	V_{REF+}	A	A	A	AN3	V_{SS}	7/1
0010	D	D	D	A	A	A	A	A	V_{DD}	V_{SS}	5/0
0011	D	D	D	A	V_{REF+}	A	A	A	AN3	V_{SS}	4/1
0100	D	D	D	D	A	D	A	A	V_{DD}	V_{SS}	3/0
0101	D	D	D	D	V_{REF+}	D	A	A	AN3	V_{SS}	2/1
011X	D	D	D	D	D	D	D	D	---	---	0/0
1000	A	A	A	A	V_{REF+}	V_{REF-}	A	A	AN3	AN2	6/2
1001	D	D	A	A	A	A	A	A	V_{DD}	V_{SS}	6/0
1010	D	D	A	A	V_{REF+}	A	A	A	AN3	V_{SS}	5/1
1011	D	D	A	A	V_{REF+}	V_{REF-}	A	A	AN3	AN2	4/2
1100	D	D	D	A	V_{REF+}	V_{REF-}	A	A	AN3	AN2	3/2
1101	D	D	D	D	V_{REF+}	V_{REF-}	A	A	AN3	AN2	2/2
1110	D	D	D	D	D	D	D	A	V_{DD}	V_{SS}	1/0
1111	D	D	D	D	V_{REF+}	V_{REF-}	D	A	AN3	AN2	½

A = Analog input D = Digital I/O

C/R = Number of analog input channels/Number of A/D voltage references

There are 16 bits in the two result registers. The AD conversion takes 10 bits. Therefore the 6 bits are used. The result format bit allows determining whether the first 6 bits of the high register are not used (right justified), or the 6 bits of the low register are not used (left justified).

To see this let us consider the binary number 11111111 (decimal 1023) obtained as a result of AD conversion. Then the justification of ADRESH:ADRESL will be

Right justified (ADFM=1)	XXXXXX11111111
Left justified (ADFM=0)	11111111XXXXXX

By assigning the values for the registers, the PIC microcontroller can be used for AD conversion. The port configuration of PIC 16F877A is shown in the figure and the assembly language code for AD conversion and gate pulse generation to the MOSFET is presented below.

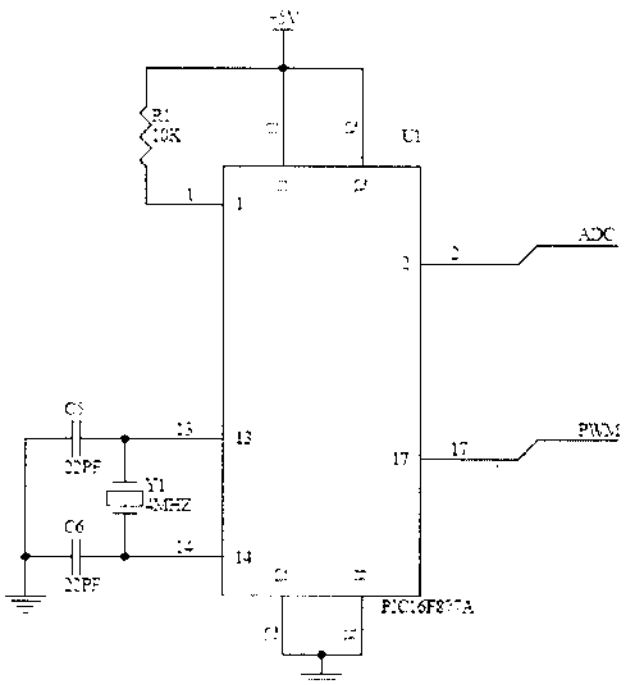

Figure 4.5 PIC circuit for triggering MOSFET of the Boost Chopper

4.4 CODING

The assembly language program is presented below:

```
#include<pic.h>
```

```
__CONFIG(WDTDIS & XT & PWRTEN & BOREN & LVPDIS);
unsigned char count;
unsigned char d_cycle;
unsigned char lookup[10]={0x3f,0x06,0x5b,0x4f,0x66,0x6d,0x7d,0x07,0xff,0x6f};
unsigned int ADRES,TEMP;
void main()
{
        ADCON1=0X8E;
        TRISA=0X01;
        PORTA=0;

        TRISB=0;
        PORTB=0;

        TRISC=0;
        PORTC=0;

        T2CON=0X04;
        PR2=99;
        CCP1CON=0X0C;
        d_cycle=CCPR1L=0X0a;

        GIE=PEIE=TMR1IE=1;
//      delay1();
//      delay1();

        while(1)
        {
                ADCON0=0X81;
                delay();
                ADGO=1;
```

```
                dclay();
                while(ADGO);
                ADRES=ADRESH*256+ADRESL;
                ADRES=ADRES/2;
                if(ADRES<460)
                {
                        d_cycle++;
                        if(d_cycle>25)
                                d_cycle=25;
                }
                if(ADRES>470)
                {
                        d_cycle--;
                        if(d_cycle<10)
                                d_cycle=10;
                }

                CCPR1L=d_cycle;
                delay1();
//              dclay1();
//              delay1();

        }
}
delay()
{
        unsigned char i;
        for(i=0;i<=100;i++);
}
delay1()
{
```

```
    unsigned int i;
    for(i=0;i<50000;i++);
}
```

Chapter 4

Gate Pulse Generation Using PIC Microcontroller

Chapter 5

Experimental Investigations

5.1 INTRODUCTION

The experimental setup of the proposed closed loop scheme is presented in this chapter. The details of the fabrication of the chopper circuit and the implementation of the MPPT algorithm using microcontroller in the feedback circuit of the chopper is described in this chapter.

5.2 EXPERIMENTAL SET-UP

The prototype model consists of boost chopper used to step up voltages to reduced levels i.e. voltages from 10V to 16V are stepped up to 49V. The complete experimental set-up of the proposed scheme shown in Figure 5.1 consists of a 12V dc source (in place of solar panel), a Boost chopper using a mosfet, PIC microcontroller (PIC16F877A) and an opto-coupler. The dc-dc converter consists of inductor of value 470mH, a Mosfet (IRFZ44), capacitor of value 220nF and a power diode (IN5819). The 12V Dc source is connected to the Boost chopper and the maximum power is tracked using the closed loop controller.

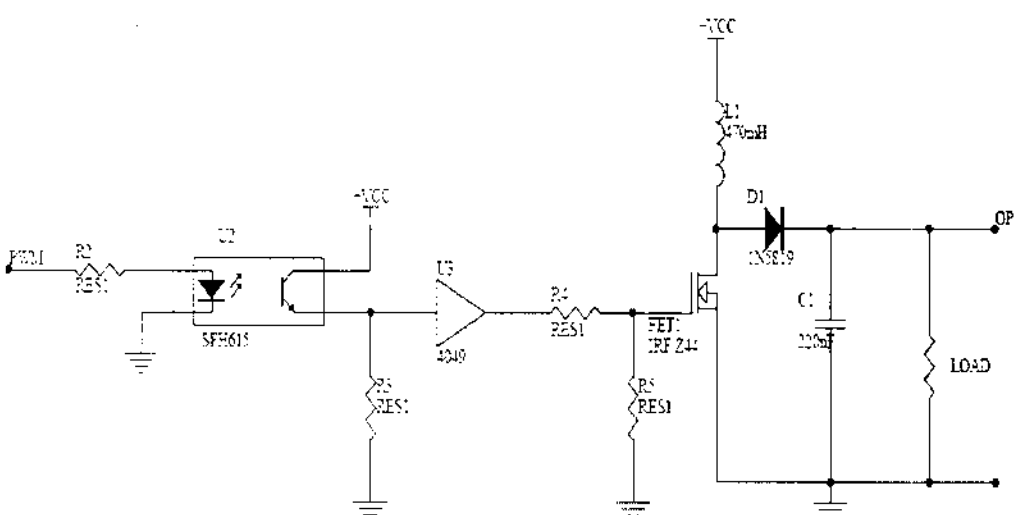

Figure 5.1 Circuit of Boost converter along with Optocoupler

An Optocoupler involves a LED and a phototransistor, separated so that light may travel across a barrier but electrical current may not. When an electrical signal is applied to the input of the opto-isolator, its LED lights, its light sensor then activates, and a corresponding electrical signal is generated at the output. Unlike a transformer, the opto-isolator allows for DC coupling and generally provides significant protection from serious overvoltage conditions in one circuit affecting the other.

The optocoupler is used in the circuit for voltage isolation between the PIC microcontroller which generates the gate pulses and the MOSFET in the chopper circuit.

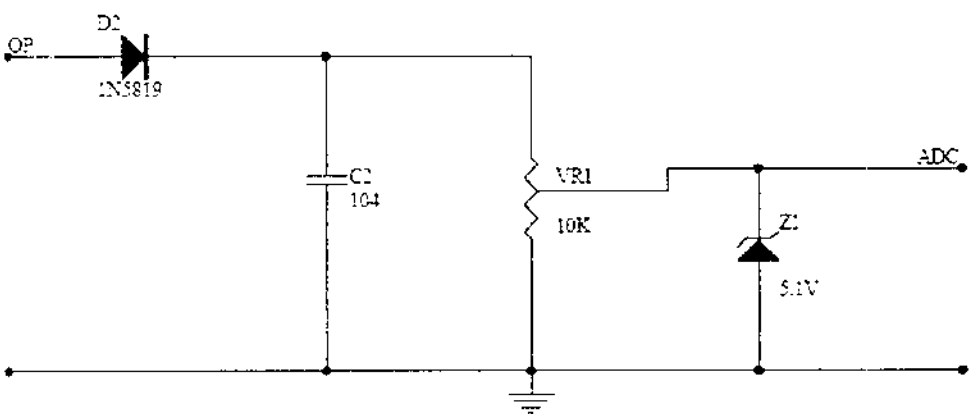

Figure 5.2 Circuit of the Potential Divider used in the feedback loop of the tracker

This circuit depicts the potential divider used in the feedback loop of the chopper circuit. A zener diode is used in the divider circuit. A Zener diode is a type of diode that permits current in the forward direction like a normal diode, but also in the reverse direction if the voltage is larger than the breakdown voltage known as "Zener knee voltage" or "Zener voltage". A reverse-biased Zener diode will exhibit a controlled breakdown and allow the current to keep the voltage across the Zener diode at the Zener voltage. A diode with a Zener breakdown voltage of 5.1 V will exhibit a voltage drop of 5.1V if the reverse bias voltage applied across it is more than its Zener

voltage.So this ensures that the voltage does not exceed the limit thus preventing damage to the microcontroller.

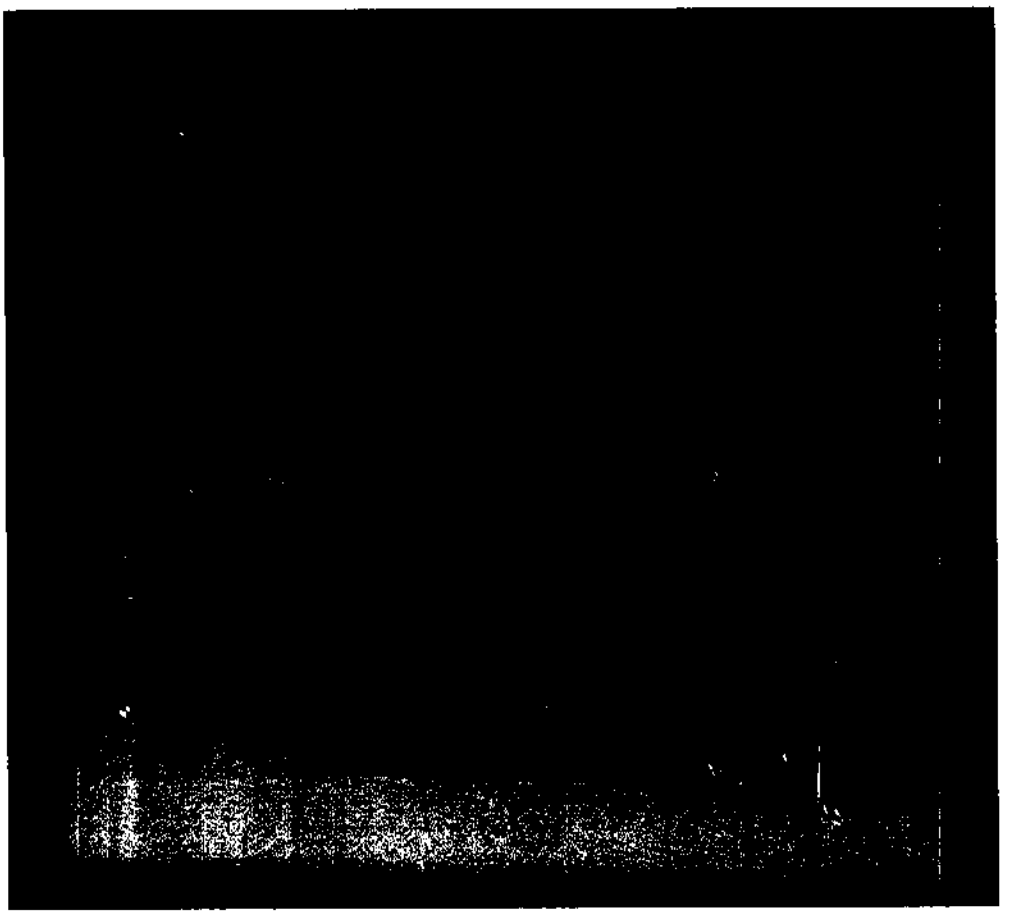

Figure 5.3 Photograph of the Boost chopper circuit controlled by MPPT algorithm implemented using PIC Microcontroller

5.3 EXPERIMENTAL RESULTS

The battery which is charged initially by the photovoltaic panel is connected to the dc-dc converter and the output of the converter can be used to drive a load. The controller for producing variation in the duty cycle has been constructed using the PIC microcontroller. For the closed loop operation of the proposed scheme an analog feedback circuit has been fabricated using the potential divider and an opto-coupler.

Depending upon the dc output of the chopper, the duty cycle is automatically adjusted in the closed loop operation of the proposed scheme for extracting maximum power. It is verified that for input voltages ranging from 10V to 16V, the output voltage is maintained at approximately 49V.

Chapter 6

Conclusion and Recommendations

6.1 CONCLUSION

A boost chopper with a closed loop control to step up voltages from lower levels stored in the battery to higher levels has been designed. The output voltage from the chopper is maintained at a constant value using the MPPT algorithm. A PIC microcontroller has been programmed to vary the duty cycle of the converter for tracking the maximum power output that is available to the load. Simulation studies of the closed loop scheme have been carried out.

The boost chopper has been fabricated using a power MOSFET together with an inductance of 470mH, a capacitor of 220nF and a power diode. The MOSFET and power diode have been mounted on a heat sink. The details of the complete setup of the closed loop scheme have been presented in the report. The gate pulses to the MOSFET have been generated using PIC 16F877A Microcontroller .The scheme of varying the duty cycle of the gate pulses along with the assembly language program has been presented. In simulation analysis, the output voltage of the Chopper is compared with the reference value determined from the panel ratings. The signal obtained is compared with saw tooth waveform and the result is used to trigger the MOSFET. The simulated waveforms and the experimental results have been verified to be similar and have been furnished in the report for verification.

6.2 SCOPE FOR FURTHER WORK

Attempts can be made to convert the dc power from the chopper to ac power so that it can be connected to ac loads or to the utility grids. The DSP processor can be used in place of PIC microcontroller for better performance and faster response.

REFERENCES

[1] Trishan Esram and Patrick L. Chapman, "Comparison of Photovoltaic Array Maximum Power Point Tracking Techniques" in IEEE Transactions on Energy Conversion, August 2005.

[2] Mehmet Bodur and Mummer Ermis, " Maximum Power Point Tracking for Low Power Photovoltaic Solar Panels", IEEE Transactions on Power Electronics, pp 758-761, 2004.

[3] Trishan Esram, Jonathan W. Kimball, Philip T. Krein, Patrick L. Chapman and Pallab Midya "Dynamic Maximum Power Point Tracking of Photovoltaic Arrays Using Ripple Correlation Control", IEEE Transactions on Power Electronics, vol. 21, no. 5, pp 1282-1291, September 2006.

[4] Muhammad H. Rashid, "Power Electronics : Circuits, Devices and Applications", Pearson Education, Third edition, 2004/PHI.

[5] Datasheet for MOSFET - IRFZ44
URL: http://www.datasheetcatalog.com/datasheets_pdf/I/R/F/Z/IRFZ44.shtml
Accessed online:10 January 2009

[6] Datasheet for Optocoupler - SFH615
URL:http://www.datasheetcatalog.com/datasheets_pdf/S/F/H/6/SFH615.shtml
Accessed online : 10 January 2009

[7] Datasheets for Schottky diode
URL: http://www.datasheetcatalog.com/datasheets_pdf/1/N/5/8/1N5817.shtml
Accessed online: 10 january 2009

Appendix

MICROCHIP

PIC16F87XA

28/40/44-Pin Enhanced Flash Microcontrollers

Devices Included in this Data Sheet:

- PIC16F873A
- PIC16F874A
- PIC16F876A
- PIC16F877A

High-Performance RISC CPU:

- Only 35 single-word instructions to learn
- All single-cycle instructions except for program branches, which are two-cycle
- Operating speed: DC – 20 MHz clock input
  DC – 200 ns instruction cycle
- Up to 8K x 14 words of Flash Program Memory, Up to 368 x 8 bytes of Data Memory (RAM), Up to 256 x 8 bytes of EEPROM Data Memory
- Pinout compatible to other 28-pin or 40/44-pin PIC16CXXX and PIC16FXXX microcontrollers

Peripheral Features:

- Timer0: 8-bit timer/counter with 8-bit prescaler
- Timer1: 16-bit timer/counter with prescaler, can be incremented during Sleep via external crystal/clock
- Timer2: 8-bit timer/counter with 8-bit period register, prescaler and postscaler
- Two Capture, Compare, PWM modules
  - Capture is 16-bit, max. resolution is 12.5 ns
  - Compare is 16-bit, max. resolution is 200 ns
  - PWM max. resolution is 10-bit
- Synchronous Serial Port (SSP) with SPI™ (Master mode) and I^2C™ (Master/Slave)
- Universal Synchronous Asynchronous Receiver Transmitter (USART/SCI) with 9-bit address detection
- Parallel Slave Port (PSP) – 8 bits wide with external $\overline{RD}$, $\overline{WR}$ and $\overline{CS}$ controls (40/44-pin only)
- Brown-out detection circuitry for Brown-out Reset (BOR)

Analog Features:

- 10-bit, up to 8-channel Analog-to-Digital Converter (A/D)
- Brown-out Reset (BOR)
- Analog Comparator module with:
  - Two analog comparators
  - Programmable on-chip voltage reference (V_{REF}) module
  - Programmable input multiplexing from device inputs and internal voltage reference
  - Comparator outputs are externally accessible

Special Microcontroller Features:

- 100,000 erase/write cycle Enhanced Flash program memory typical
- 1,000,000 erase/write cycle Data EEPROM memory typical
- Data EEPROM Retention > 40 years
- Self-reprogrammable under software control
- In-Circuit Serial Programming™ (ICSP™) via two pins
- Single-supply 5V In-Circuit Serial Programming
- Watchdog Timer (WDT) with its own on-chip RC oscillator for reliable operation
- Programmable code protection
- Power saving Sleep mode
- Selectable oscillator options
- In-Circuit Debug (ICD) via two pins

CMOS Technology:

- Low-power, high-speed Flash/EEPROM technology
- Fully static design
- Wide operating voltage range (2.0V to 5.5V)
- Commercial and Industrial temperature ranges
- Low-power consumption

Device	Program Memory		Data SRAM (Bytes)	EEPROM (Bytes)	I/O	10-bit A/D (ch)	CCP (PWM)	MSSP		USART	Timers 8/16-bit	Comparators
	Bytes	# Single Word Instructions						SPI	Master I^2C			
PIC16F873A	7.2K	4096	192	128	22	5	2	Yes	Yes	Yes	2/1	2
PIC16F874A	7.2K	4096	192	128	33	8	2	Yes	Yes	Yes	2/1	2
PIC16F876A	14.3K	8192	368	256	22	5	2	Yes	Yes	Yes	2/1	2
PIC16F877A	14.3K	8192	368	256	33	8	2	Yes	Yes	Yes	2/1	2

Pin Diagrams

28-Pin PDIP, SOIC, SSOP

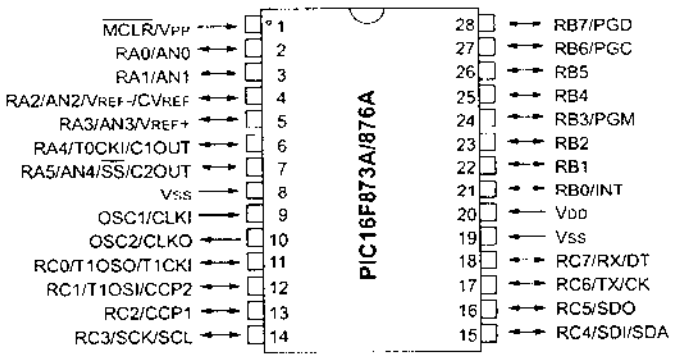

28-Pin QFN

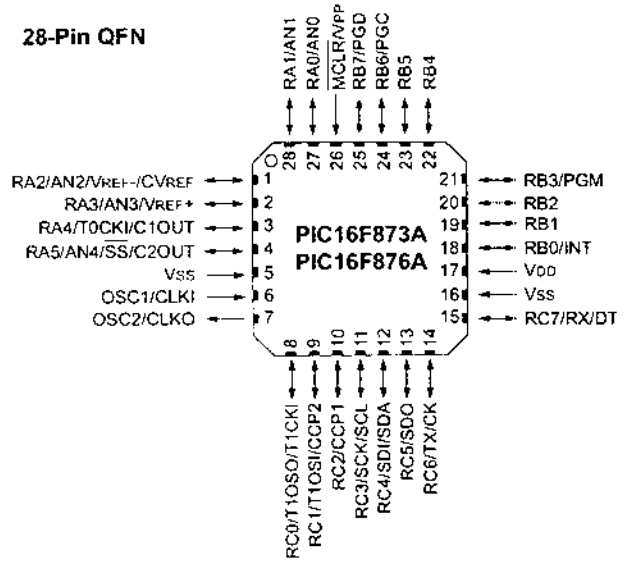

44-Pin QFN

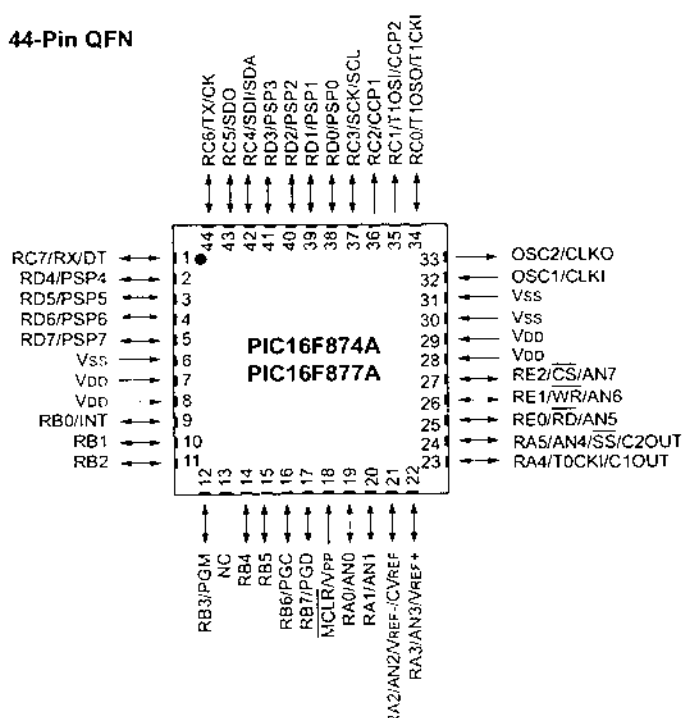

Pin Diagrams (Continued)

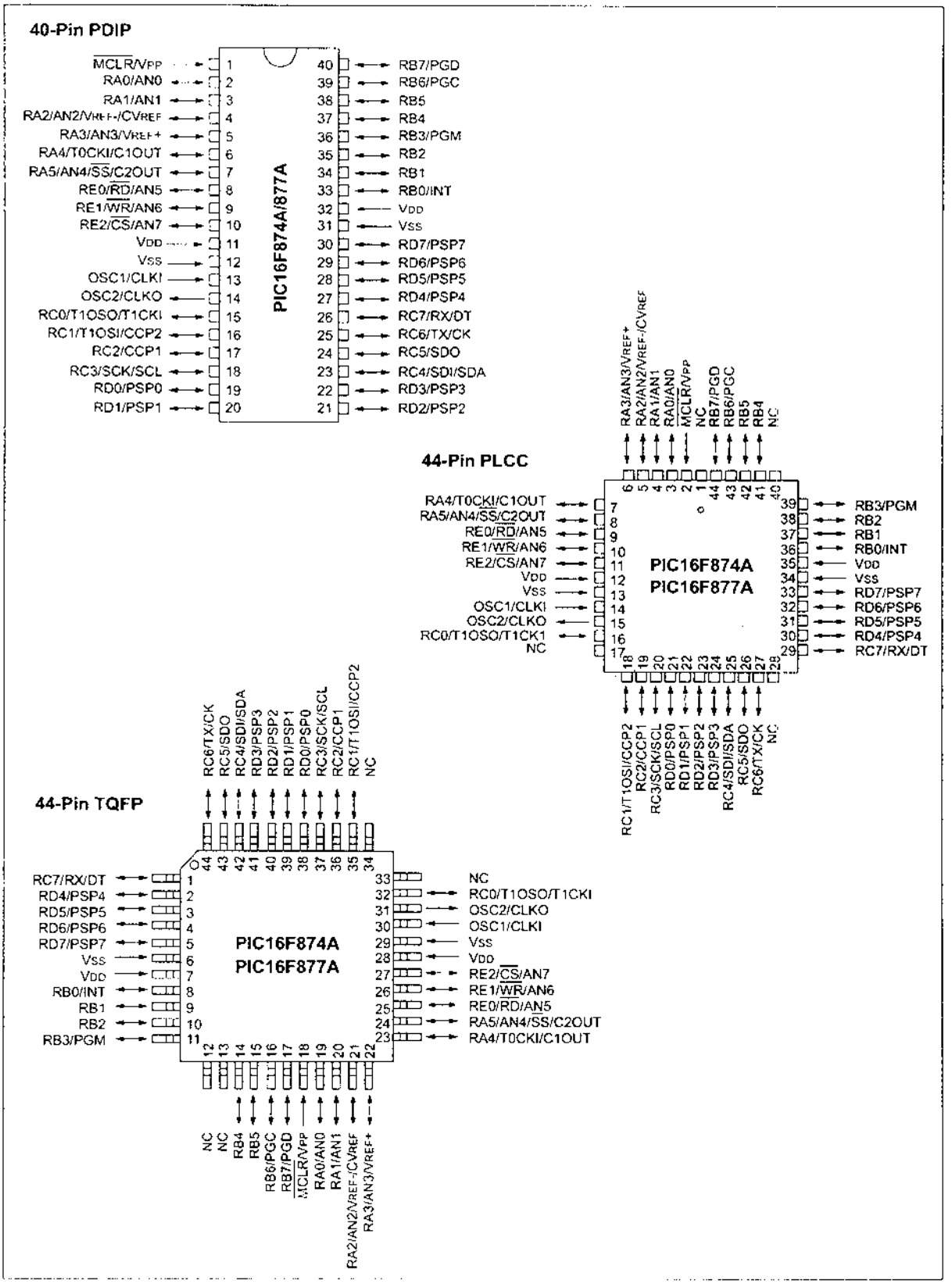

International IOR Rectifier

IRFZ44

HEXFET® Power MOSFET

- Dynamic dv/dt Rating
- 175°C Operating Temperature
- Fast Switching
- Ease of Paralleling
- Simple Drive Requirements

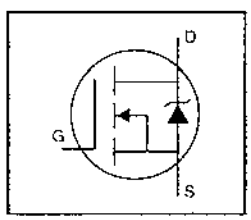

V_{DSS} = 60V

$R_{DS(on)}$ = 0.028Ω

I_D = 50*A

Description

Third Generation HEXFETs from International Rectifier provide the designer with the best combination of fast switching, ruggedized device design, low on-resistance and cost-effectiveness.

The TO-220 package is universally preferred for all commercial-industrial applications at power dissipation levels to approximately 50 watts. The low thermal resistance and low package cost of the TO-220 contribute to its wide acceptance throughout the industry.

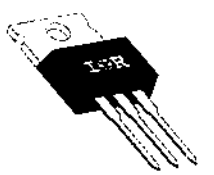

TO-220AB

DATA SHEETS

Absolute Maximum Ratings

	Parameter	Max.	Units
I_D @ T_C = 25°C	Continuous Drain Current, V_{GS} @ 10 V	50*	A
I_D @ T_C = 100°C	Continuous Drain Current, V_{GS} @ 10 V	36	
I_{DM}	Pulsed Drain Current ①	200	
P_D @ T_C = 25°C	Power Dissipation	150	W
	Linear Derating Factor	1.0	W/°C
V_{GS}	Gate-to-Source Voltage	±20	V
E_{AS}	Single Pulse Avalanche Energy ②	100	mJ
dv/dt	Peak Diode Recovery dv/dt ③	4.5	V/ns
T_J	Operating Junction and	-55 to +175	°C
T_{STG}	Storage Temperature Range		
	Soldering Temperature, for 10 seconds	300 (1.6mm from case)	
	Mounting Torque, 6-32 or M3 screw	10 lbf-in (1.1 N-m)	

Thermal Resistance

	Parameter	Min.	Typ.	Max.	Units
R_{thJC}	Junction-to-Case	—	—	1.0	°C/W
R_{thCS}	Case-to-Sink, Flat, Greased Surface	—	0.50	—	
R_{thJA}	Junction-to-Ambient	—	—	62	

Electrical Characteristics @ T_J = 25°C (unless otherwise specified)

	Parameter	Min.	Typ.	Max.	Units	Test Conditions
$V_{(BR)DSS}$	Drain-to-Source Breakdown Voltage	60	—	—	V	V_{GS}=0V, I_D= 250µA
$\Delta V_{(BR)DSS}/\Delta T_J$	Breakdown Voltage Temp. Coefficient	—	0.060	—	V/°C	Reference to 25°C, I_D= 1mA
$R_{DS(on)}$	Static Drain-to-Source On-Resistance	—	—	0.028	Ω	V_{GS}=10V, I_D=31A ④
$V_{GS(th)}$	Gate Threshold Voltage	2.0	—	4.0	V	V_{DS}=V_{GS}, I_D= 250µA
g_{fs}	Forward Transconductance	15	—	—	S	V_{DS}=25V, I_D=31A ④
I_{DSS}	Drain-to-Source Leakage Current	—	—	25	µA	V_{DS}=60V, V_{GS}=0V
		—	—	250		V_{DS}=48V, V_{GS}=0V, T_J=150°C
I_{GSS}	Gate-to-Source Forward Leakage	—	—	100	nA	V_{GS}=20V
	Gate-to-Source Reverse Leakage	—	—	-100		V_{GS}=-20V
Q_g	Total Gate Charge	—	—	67	nC	I_D=51A
Q_{gs}	Gate-to-Source Charge	—	—	18		V_{DS}=48V
Q_{gd}	Gate-to-Drain ("Miller") Charge	—	—	25		V_{GS}=10V See Fig. 6 and 13 ④
$t_{d(on)}$	Turn-On Delay Time	—	14	—	ns	V_{DD}=30V
t_r	Rise Time	—	110	—		I_D=51A
$t_{d(off)}$	Turn-Off Delay Time	—	45	—		R_G=9.1Ω
t_f	Fall Time	—	92	—		R_D=0.55Ω See Figure 10 ④
L_D	Internal Drain Inductance	—	4.5	—	nH	Between lead, 6 mm (0.25in.) from package and center of die contact
L_S	Internal Source Inductance	—	7.5	—		
C_{iss}	Input Capacitance	—	1900	—	pF	V_{GS}=0V
C_{oss}	Output Capacitance	—	920	—		V_{DS}=25V
C_{rss}	Reverse Transfer Capacitance	—	170	—		f=1.0MHz See Figure 5

Source-Drain Ratings and Characteristics

	Parameter	Min.	Typ.	Max.	Units	Test Conditions
I_S	Continuous Source Current (Body Diode)	—	—	50*	A	MOSFET symbol showing the integral reverse p-n junction diode.
I_{SM}	Pulsed Source Current (Body Diode) ①	—	—	200		
V_{SD}	Diode Forward Voltage	—	—	2.5	V	T_J=25°C, I_S=51A, V_{GS}=0V ④
t_{rr}	Reverse Recovery Time	—	120	180	ns	T_J=25°C, I_F=51A
Q_{rr}	Reverse Recovery Charge	—	0.53	0.80	µC	di/dt=100A/µs ④
t_{on}	Forward Turn-On Time	Intrinsic turn-on time is neglegible (turn-on is dominated by L_S+L_D)				

Notes:

① Repetitive rating; pulse width limited by max. junction temperature (See Figure 11)

② V_{DD}=25V, starting T_J=25°C, L=44µH R_G=25Ω, I_{AS}=51A (See Figure 12)

③ I_{SD}≤51A, di/dt≤250A/µs, V_{DD}≤$V_{(BR)DSS}$, T_J≤175°C

④ Pulse width ≤ 300 µs; duty cycle ≤2%.

* Current limited by the package, (Die Current = 51A)

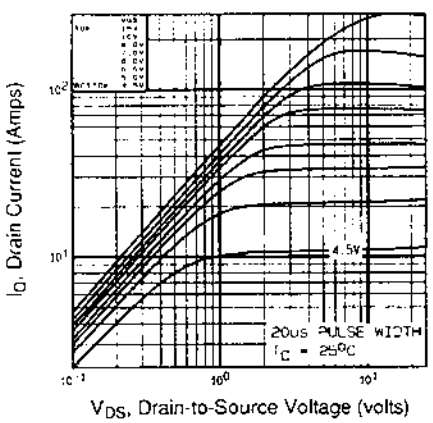

Fig 1. Typical Output Characteristics, T_C=25°C

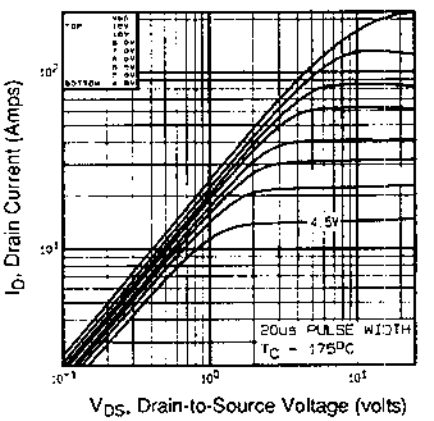

Fig 2. Typical Output Characteristics, T_C=175°C

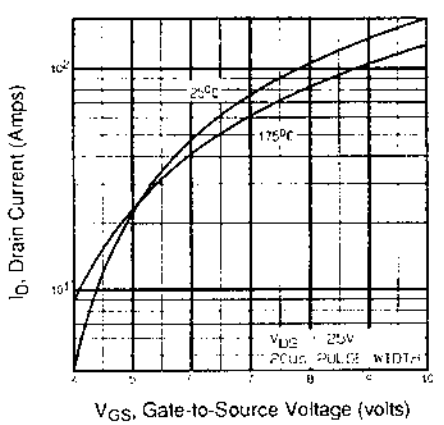

Fig 3. Typical Transfer Characteristics

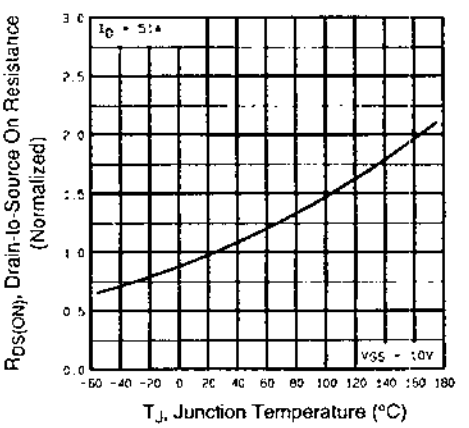

Fig 4. Normalized On-Resistance Vs. Temperature

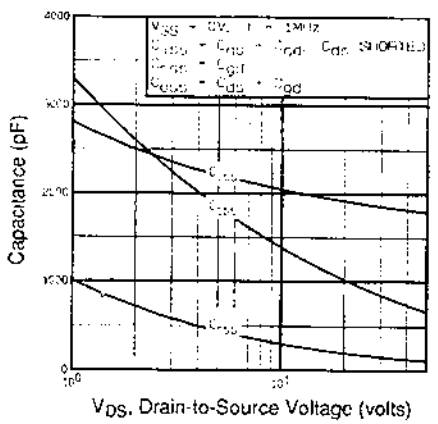

Fig 5. Typical Capacitance Vs. Drain-to-Source Voltage

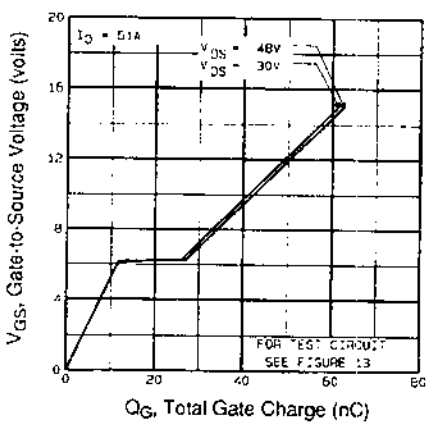

Fig 6. Typical Gate Charge Vs. Gate-to-Source Voltage

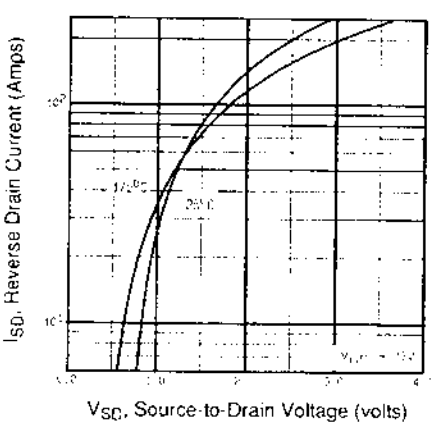

Fig 7. Typical Source-Drain Diode Forward Voltage

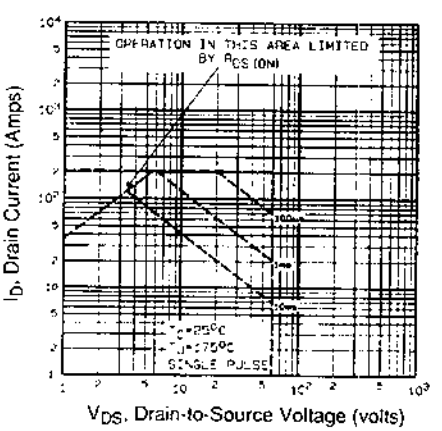

Fig 8. Maximum Safe Operating Area

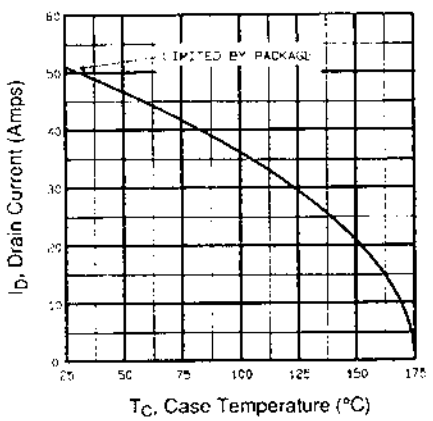

Fig 9. Maximum Drain Current Vs. Case Temperature

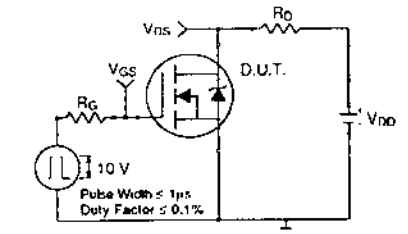

Fig 10a. Switching Time Test Circuit

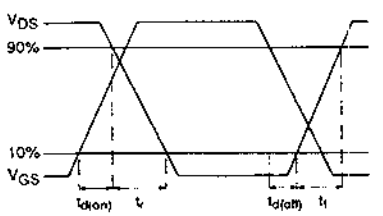

Fig 10b. Switching Time Waveforms

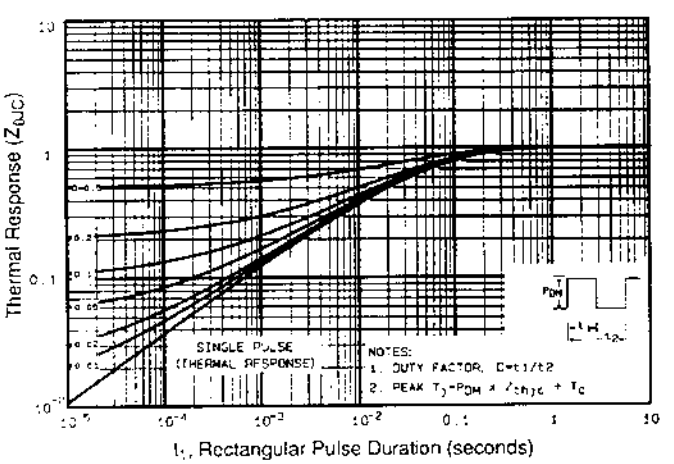

Fig 11. Maximum Effective Transient Thermal Impedance, Junction-to-Case

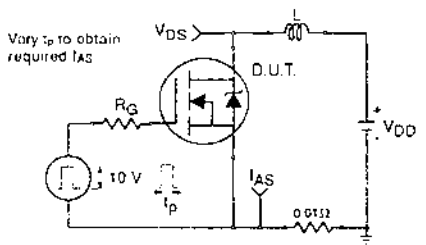

Fig 12a. Unclamped Inductive Test Circuit

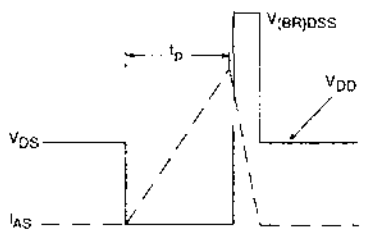

Fig 12b. Unclamped Inductive Waveforms

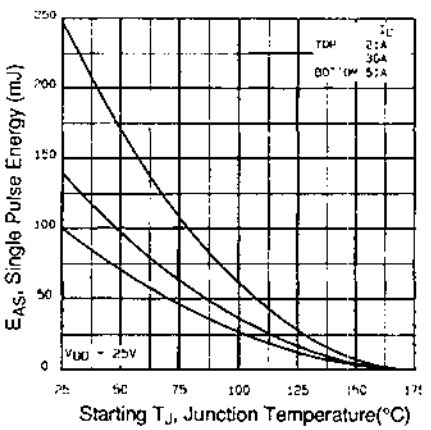

Fig 12c. Maximum Avalanche Energy Vs. Drain Current

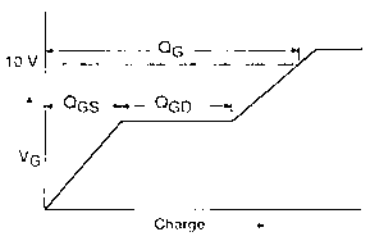

Fig 13a. Basic Gate Charge Waveform

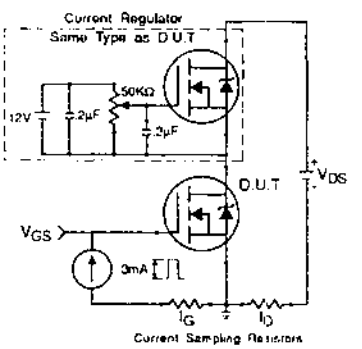

Fig 13b. Gate Charge Test Circuit

Appendix A: Figure 14, Peak Diode Recovery dv/dt Test Circuit – See page 1505

Appendix B: Package Outline Mechanical Drawing – See page 1509

Appendix C: Part Marking Information – See page 1516

Appendix E: Optional Leadforms – See page 1525

International IOR Rectifier

1N 5817 ...1N 5819
SCHOTTKY BARRIER DIODE

Features

- Plastic package has Underwriters Laboratory Flammability Classification 94V-0
- Metal silicon junction, majority carrier conduction
- Guardring for overvoltage protection
- Low power loss, high efficiency
- High current capability low forward voltage drop
- High surge capability
- For use in low voltage, high frequency inverters, free wheeling, and polarity protection applications
- High temperature soldering guaranteed: 250 °C/10 seconds, 0.375" (9.5mm) lead length, 5 lbs. (2.3 Kg) tension

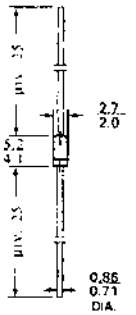

Dimensions in mm

Weight Approx. 0.34g

Maximum Ratings and Electrical Characteristics

Ratings at 25 °C ambient temperature unless otherwise specified.

Characteristic	Symbols	1N5817	1N5818	1N5819	Units
* Maximum repetitive peak reverse voltage	V_{RRM}	20	30	40	Volts
Maximum RMS voltage	V_{RMS}	14	21	28	Volts
* Maximum DC blocking voltage	V_{DC}	20	30	40	Volts
* Maximum non-repetitive peak reverse voltage	V_{RSM}	24	36	48	Volts
* Maximum average forward rectified current 0.375" (9.5mm) lead length at T_L=90 °C	$I_{(AV)}$	1.0			Amp
* Peak forward surge current, 8.3ms single half sine-wave superimposed on rated load (JEDEC Method) at T_L=70 °C	I_{FSM}	25.0			Amp
* Maximum instantaneous forward voltage at 1.0A (NOTE 1) * Maximum instantaneous forward voltage at 3.1A (NOTE 1)	V_F V_F	0.450 0.750	0.550 0.875	0.600 0.900	Volts Volts
* Maximum instantaneous reverse current at T_A=25 °C (NOTE 1) rated DC reverse voltage T_A=100 °C	I_R	1.0 10.0			mA
Typical thermal resistance (NOTE 2)	$R_{\theta JA}$ $R_{\theta JL}$	50.0 15.0			°C/W
Typical junction capacitance (NOTE 3)	C_J	110.0			pF
* Storage and operating junction temperature range	T_J, T_{STG}	-65 to + 125			°C

1N 5817 ...1N 5819
SCHOTTKY BARRIER DIODE

FIG. 1-FORWARD CURRENT DERATING CURVE

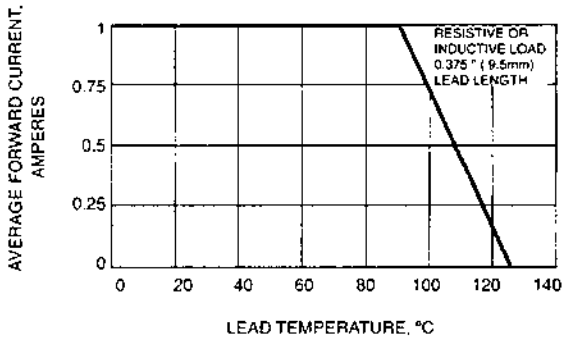

FIG. 2-MAXIMUM NON-REPETITIVE PEAK FORWARD SURGE CURRENT

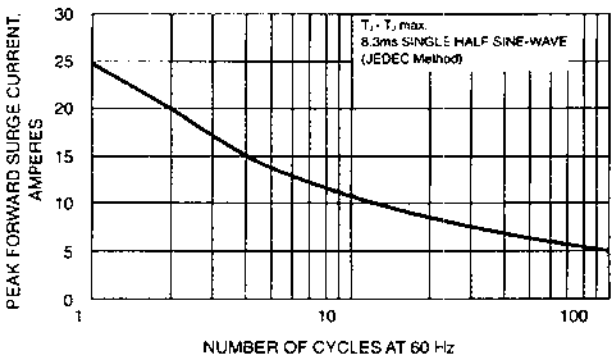

FIG. 3-TYPICAL INSTANTANEOUS FORWARD CHRACTERISTICS

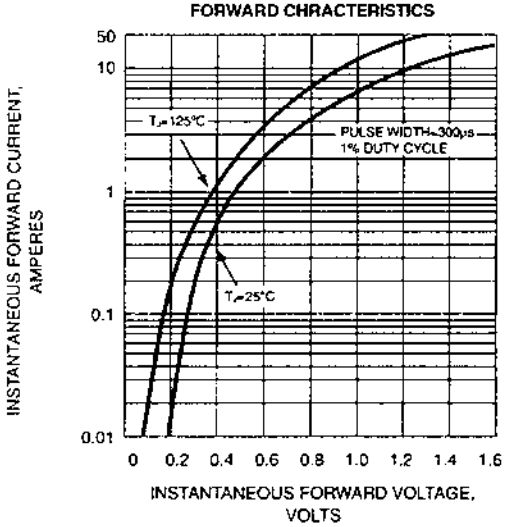

FIG. 4-TYPICAL REVERSE CHARACTERISTICS

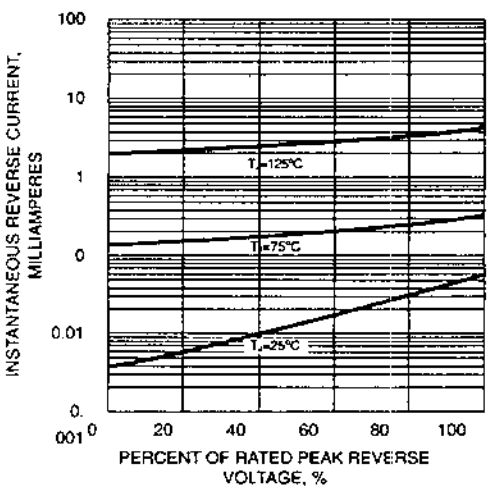

FIG. 5-TYPICAL JUNCTION CAPACITANCE

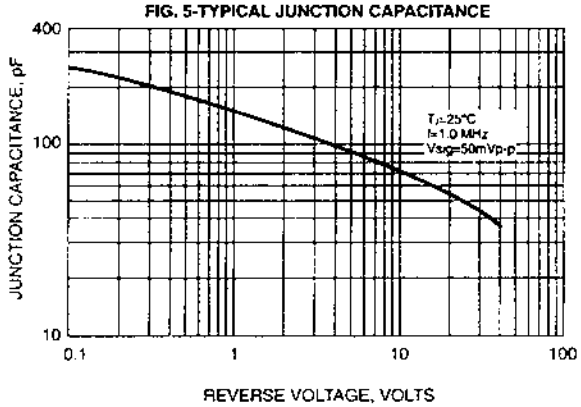

FIG. 6-TYPICAL TRANSIENT THERMAL IMPEDANCE

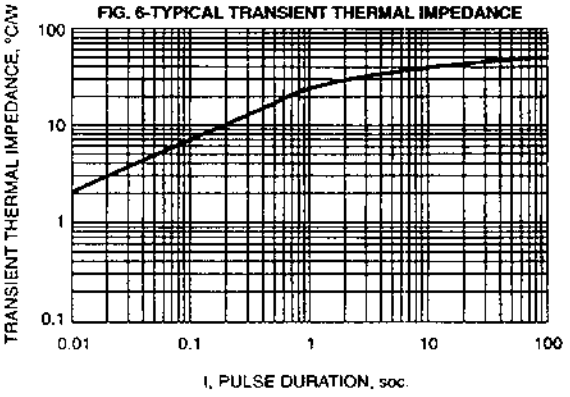

SIEMENS

SFH 610
SFH 611
SFH 615

2.8 kV TRIOS® OPTOCOUPLERS
HIGH RELIABILITY

T-41-83

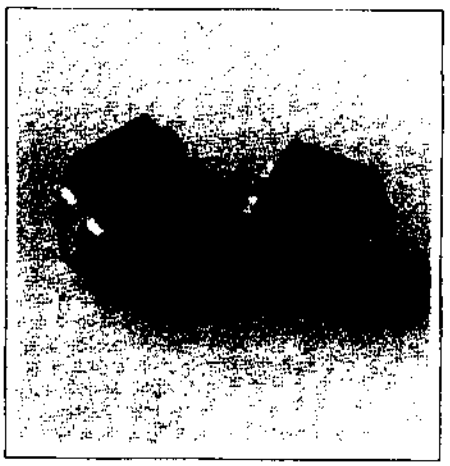

Package Dimensions mm

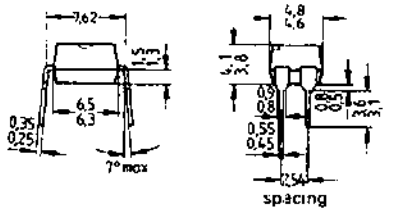

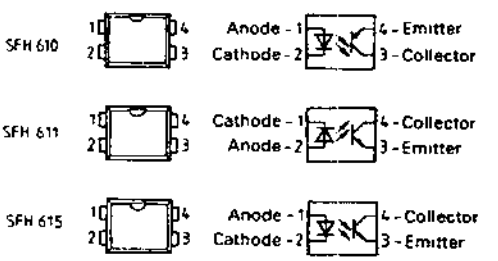

FEATURES

- **Isolation Test Voltage: 2800 V**
- **High Current Transfer Ratios at 10 mA: 40-320% at 1 mA: 60% typical (>13)**
- **Fast Switching Times**
- **Minor CTR Degradation**
- **100% Burn-In**
- **Field-Effect Stable by TRIOS**
- **Temperature Stable**
- **Good CTR Linearity Depending on Forward Current**
- **High Collector-Emitter Voltage V_{CEO}=70 V**
- **Low Saturation Voltage**
- **Low Coupling Capacitance**
- **End-Stackable in 2.54 mm Spacing**
- **High Common-Mode Interference Immunity (Unconnected Base)**
- **UL Approval #52744**
- **VDE Approval 0883**
- **VDE Approval 0884 (Optional with Option 1)**

DESCRIPTION

The optically coupled isolators SFH 610, SFH 611 and SFH 615 feature a high current transfer ratio, low coupling capacitance and high isolation test voltage. They employ a GaAs LED as emitter, which is optically coupled with a silicon planar phototransistor as detector.

The components are incorporated in a plastic plug-in DIP-4 package.

The coupling devices are designed for signal transmission between two electrically separated circuits. The potential difference between the circuits to be coupled is not allowed to exceed the maximum permissible reference voltages.

The couplers are end-stackable in a 2.54 mm spacing and are considered as successor types for the couplers in metal case. The SFH 610, SFH 611 and SFH 615 differ in their arrangement of the terminal pins. Multicouplers can thus easily be implemented and conventional multicouplers can be replaced.

*TRansparent IOn Shield

Maximum Ratings

Emitter (GaAs LED)

Reverse Voltage	6 V
DC Forward Current	60 mA
Surge Forward Current (t≤10 µs)	2.5 A
Total Power Dissipation	100 mW

Detector (Silicon Phototransistor)

Collector-Emitter Voltage	70 V
Collector Current	50 mA
Collector Current (t ≤ 1 ms)	100 mA
Total Power Dissipation	150 mW

Optocoupler

Storage Temperature Range	-55°C to +150°C
Ambient Temperature Range	-55°C to +100°C
Junction Temperature	100°C
Soldering Temperature (max. 10 s)[1]	260°C
Isolation Test Voltage[2] (between emitter and detector referred to standard climate 23/50 DIN 50014)	2800 VDC
Isolation Resistance (V_{IO}=500 V)	10^{11} Ω

Notes:
1 Dip soldering: minimum clearance from bottom edge of package 1.5 mm. Special soldering conditions apply when through-contacted circuit boards are used. Please request appropriate specification.
2 DC test voltage in accordance with DIN 57883, draft 4/78

Characteristics (T_A=25°C)

Emitter (GaAs LED)			
Forward Voltage (I_F=60 mA)	V_F	1.25 (≤1.65)	V
Breakdown Voltage (I_R=10 µA)	V_{BR}	30 (≥6)	V
Reverse Current (V_R=6 V)	I_R	0.01 (≤10)	µA
Capacitance (V_R=0 V, f=1 MHz)	C_0	25	pF
Thermal Resistance	R_{thJA}	750	K/W
Detector (Silicon Phototransistor)			
Capacitance (V_{CE}=5 V, f=1 MHz)	C_{CE}	6.8	pF
Thermal Resistance	R_{thJA}	500	K/W
Optocoupler			
Collector-Emitter Saturation Voltage (I_F=10 mA, I_C=2.5 mA)	V_{CEsat}	0.25 (≤0.4)	V
Coupling Capacitance	C_k	0.25	pF

The optocouplers are grouped according to their current transfer ratio I_C/I_F at V_{CE}=5 V, marked by dash numbers

	-1	-2	-3	-4	
I_C/I_F (I_F=10 mA)	40–80	63–125	100–200	160–320	%
I_C/I_F (I_F=1 mA)	30 (>13)	45 (>22)	70 (>34)	90 (>56)	%
Collector-Emitter Leakage Current (V_{CE}=10 V) (I_{CEO})	2 (≤50)	2 (≤50)	5 (≤100)	5 (≤100)	nA

SWITCHING TIMES

Linear Operation (without saturation)

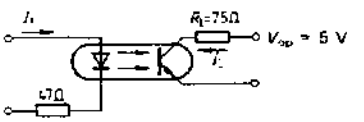

I_F=10 mA, V_{OP}=5 V, T_A=25°C

Load Resistance	R_L	75	Ω
Turn-On Time	t_{on}	3.0 (≤5.6)	µs
Rise Time	t_r	2.0 (≤4.0)	µs
Turn-Off Time	t_{off}	2.3 (≤4.1)	µs
Fall Time	t_f	2.0 (≤2.5)	µs
Cut-Off Frequency	F_{CO}	250	kHz

Switching Operation (with saturation)

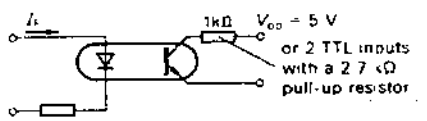

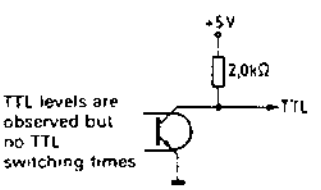

Group	-1 (I_F=20 mA)	-2 and -3 (I_F=10 mA)	-4 (I_F=5 mA)	
Turn-On Time t_{on}	3.0 (≤5.5)	4.2 (≤8.0)	6.0 (≤10.5)	µs
Rise Time t_r	2.0 (≤4.0)	3.0 (≤6.0)	4.5 (≤8.0)	µs
Turn-Off Time t_{off}	18 (≤34)	23 (≤39)	25 (≤43)	µs
Fall Time t_f	11 (≤20)	14 (≤24)	15 (≤26)	µs
V_{CEsat}	0.25 (≤0.4)			V

Current transfer ratio (typ.) versus temperature
(I_F= 10 mA, V_{CE}= 5 V)

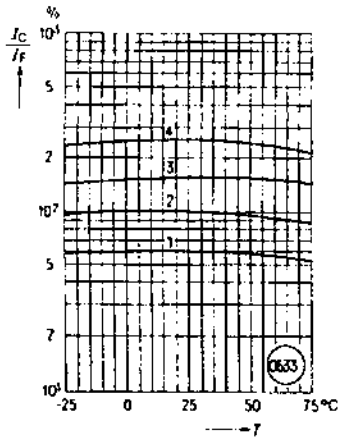

Minimum current transfer ratio versus diode forward current
(T_A=25°C, V_{CE}=5 V)

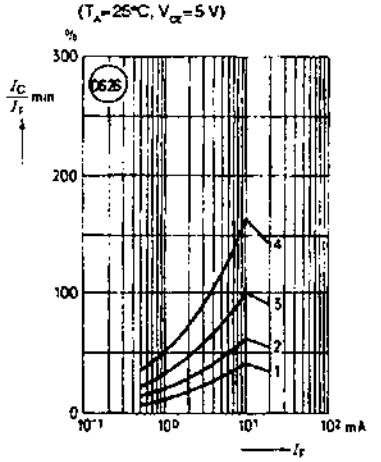

Output characteristics (typ.) Collector current versus collector-emitter voltage
(T_A=25°C)

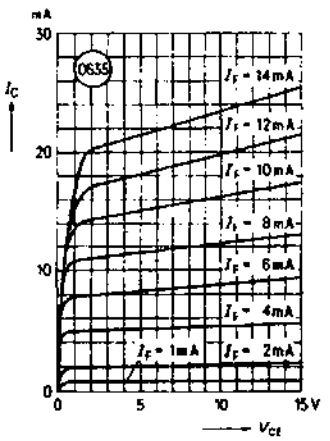

Diode forward voltage (typ.) versus forward current

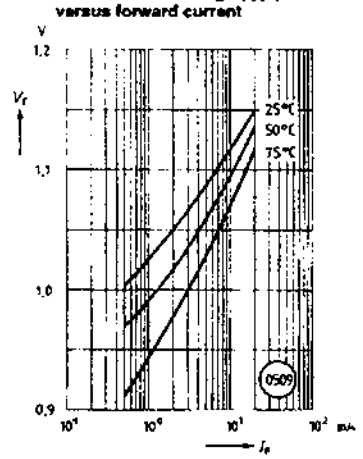

Transistor capacitance (typ.) versus collector-emitter voltage
(T_A=25°C, f= 1 MHz)

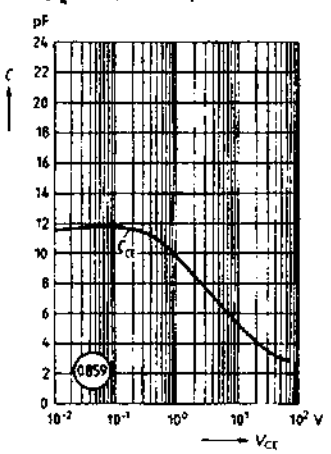

Permissible pulse handling capability Forward current versus pulse width
(D = parameter, T_A=25°C)

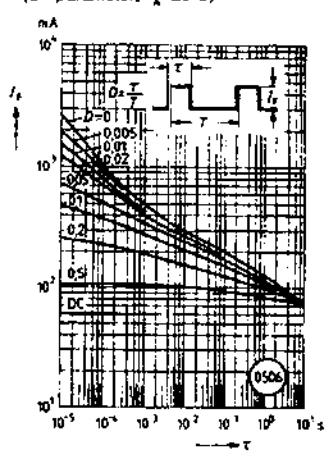

Permissible power dissipation versus ambient temperature

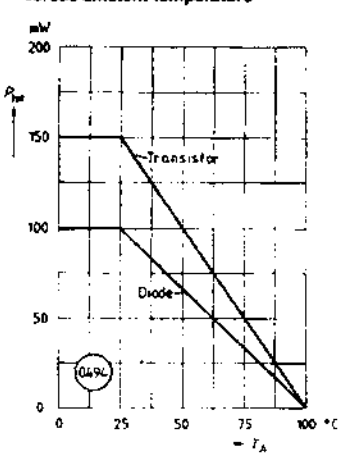

Permissible forward current of the diode versus ambient temperature

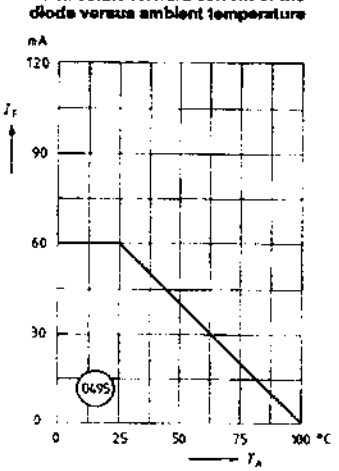

Current transfer ratio versus load time
(V_{CE}=5 V, R_L=1 kΩ, T_A=60°C, I_F=60 mA, Measuring current=10 mA, Confidence coefficient S=60%)